Journal of Polymers and the Environment, Vol. 9, No. 2, April 2001 (© 2002)

A Literature Review of Poly(Lactic Acid)

Donald Garlotta[1]

A literature review is presented regarding the synthesis, and physicochemical, chemical, and mechanical properties of poly(lactic acid)(PLA). Poly(lactic acid) exists as a polymeric helix, with an orthorhombic unit cell. The tensile properties of PLA can vary widely, depending on whether or not it is annealed or oriented or what its degree of crystallinity is. Also discussed are the effects of processing on PLA. Crystallization and crystallization kinetics of PLA are also investigated. Solution and melt rheology of PLA is also discussed. Four different power-law equations and 14 different Mark–Houwink equations are presented for PLA. Nuclear magnetic resonance, UV–VIS, and FTIR spectroscopy of PLA are briefly discussed. Finally, research conducted on starch–PLA composites is introduced.

KEY WORDS: Poly(lactic acid); synthesis; crystallization kinetics; viscosity; composites.

INTRODUCTION

Poly(lactic acid) (PLA) belongs to the family of aliphatic polyesters commonly made from α-hydroxy acids, which include polyglycolic acid or polymandelic acid, and are considered biodegradable and compostable. PLA is a thermoplastic, high-strength, high-modulus polymer that can be made from annually renewable resources to yield articles for use in either the industrial packaging field or the biocompatible/bioabsorbable medical device market. It is easily processed on standard plastics equipment to yield molded parts, film, or fibers [1]. It is one of the few polymers in which the stereochemical structure can easily be modified by polymerizing a controlled mixture of the L- or D-isomers to yield high-molecular-weight amorphous or crystalline polymers that can be used for food contact and are generally recognized as safe (GRAS) [2]. PLA is degraded by simple hydrolysis of the ester bond and does not require the presence of enzymes to catalyze this hydrolysis. The rate of degradation is dependent on the size and shape of the article, the isomer ratio, and the temperature of hydrolysis [1].

In order for PLA to be processed on large-scale production lines in applications such as injection molding, blow molding, thermoforming, and extrusion, the polymer must possess adequate thermal stability to prevent degradation and maintain molecular weight and properties. PLA undergoes thermal degradation at temperatures above 200°C (392°F) [3] by hydrolysis, lactide reformation, oxidative main chain scission, and inter- or intramolecular transesterification reactions. PLA degradation is dependent on time, temperature, low-molecular-weight impurities, and catalyst concentration [3]. Catalysts and oligomers decrease the degradation temperature and increase the degradation rate of PLA. In addition, they can cause viscosity and rheological changes, fuming during processing, and poor mechanical properties.

Poly(lactic acid) homopolymers have a glass-transition and melt temperature of about 55°C and 175°C, respectively. They require processing temperatures in excess of 185–190°C [4]. At these temperatures, unzipping and chain scission reactions leading to loss of molecular weight, as well as thermal degradations, are

[1] Plant Polymer Research Unit, National Center for Agricultural Utilization Research, USDA-ARS, 1815 North University Street, Peoria, Illinois, 61604.

1566-2543/01/0400-0063/0

known to occur. Consequently, PLA homopolymers have a very narrow processing window. The most widely used method for improving PLA processability is based on melting point depression by the random incorporation of small amounts of lactide enantiomers of opposite configuration into the polymer (i.e., adding a small amount of D-lactide to the L-lactide to obtain PDLLA). Unfortunately, the melting point depression is accompanied by a significant decrease in crystallinity and crystallization rates [4].

High-molecular-weight poly(lactic acid) is a colorless, glossy, stiff thermoplastic polymer with properties similar to polystyrene. The amorphous PLA is soluble in most organic solvents such as tetrahydrofuran (THF), chlorinated solvents, benzene, acetonitrile, and dioxane [1]. From solubility studies done at the USDA-ARS-NCAUR, the poly(lactic acid) supplied by Cargill was soluble in benzene, chloroform, 1,4-dioxane, and THF. The most appropriate solvent found so far to date for Multi-Angle Laser Light Scattering (MALLS) is 1,1,1,3,3,3-hexafluoro-2-propanol (HFIP). This is due to the acceptable difference in refractive index values between PLA (1.44) and HFIP (1.275). Poly(lactic acid), contrary to what is reported in the literature, is insoluble in acetonitrile. Crystalline PLA is soluble in chlorinated solvents and benzene at elevated temperatures. Poly(lactic acid) can be crystallized by slow cooling, annealing it above the T_g, or strain crystallized [1].

Poly(lactic acid) can be a well-behaved thermoplastic with a reasonable shelf life for most single-use packaging applications and, when disposed of properly, will hydrolyze to harmless, natural products. It could be a technical and economic solution to the problem of the eventual disposal of the very large amount of plastic packaging used in this country. In 1993, some 17.3 billion pounds of disposable plastic packaging was sold in the United States [5]. A small but significant percentage of this is disposed of as litter, which becomes a blot on the landscape and a threat to marine life. Mortality estimates are as high as 100,000 marine animals and 1 to 2 million sea birds per year. PLA has a degradation time in the environment on the order of six months to two years, which compares to 500 to 1000 years for conventional plastics such as polystyrene (PS) and polyethylene (PE) [5].

SYNTHESIS OF POLY(LACTIC ACID)

The basic building block for PLA is lactic acid, which was first isolated in 1780 from sour milk by the Swedish chemist Scheele and first produced commercially in 1881 [1]. Food-related applications are the major use of lactic acid in the United States and account for about 85% of the commercially produced product. It is used as a buffering agent, acidic flavoring agent, acidulant, and bacterial inhibitor in many processed foods. Lactic acid can be manufactured either by carbohydrate fermentation or chemical synthesis, although fermentation predominates [6–8].

Lactic acid (2-hydroxy propionic acid) is the simplest hydroxy acid with an asymmetric carbon atom and exists in two optically active configurations. The L(+)-isomer is produced in humans and other mammals, whereas both the D(−)- and L(+)-enantiomers are produced in bacterial systems. The majority of the world's commercially produced lactic acid is made by the bacterial fermentation of carbohydrates, using homolactic organisms such as various optimized or modified strains of the genus *Lactobacilli*, which exclusively form lactic acid [1]. The organisms that predominantly yield the L(+)-isomer are *Lactobacilli amylophilus*, *L. bavaricus*, *L. casei*, *L. maltaromicus*, and *L. salivarius*. Strains such as *L. delbrueckii*, *L. jensenii*, or *L. acidophilus* yield the D-isomer or mixtures of both [1]. These bacteria are classified as homofermentive, produce lactic acid through the Embden–Meyerhof pathway, and convert as much as 1.8 mole of lactic acid per mole of hexose (>90% yield lactic acid from glucose). These strains yield high carbon conversions from feed stocks at standard fermentation conditions, such as relatively low to neutral pH, temperatures around 40°C, and low oxygen concentrations [9].

The various types of carbohydrates that can be utilized in the fermentation depend on the particular strain of *Lactobacillus*. In general, most of the simple sugars obtained from agricultural byproducts can be used. These sugars include (1) glucose, maltose, and dextrose from corn or potato starch; (2) sucrose from cane or beet sugar; and (3) lactose from cheese whey. Along with the carbohydrates, the organisms require proteins and other complex nutrients such as B-vitamins, amino acids, and nucleotides, which can be supplied by corn steep liquor, yeast extract, cottonseed flour, or soy flour. These requirements are very species-dependent, and it is typical to develop the strains around the available nutrients, since these can add considerable cost to the process [6, 8, 9].

Commercial fermentation is usually conducted in a batch process, which takes three–six days to complete. Sugar concentrations of 5–10% are used, which give production rates of 2 grams of acid per 1 liter of broth per hour. A high final lactic acid concentration is desired in the final broth to give the greatest process efficiencies, but high concentrations lead to lactic acid toxicity and growth inhibition. In order to have high efficiencies and

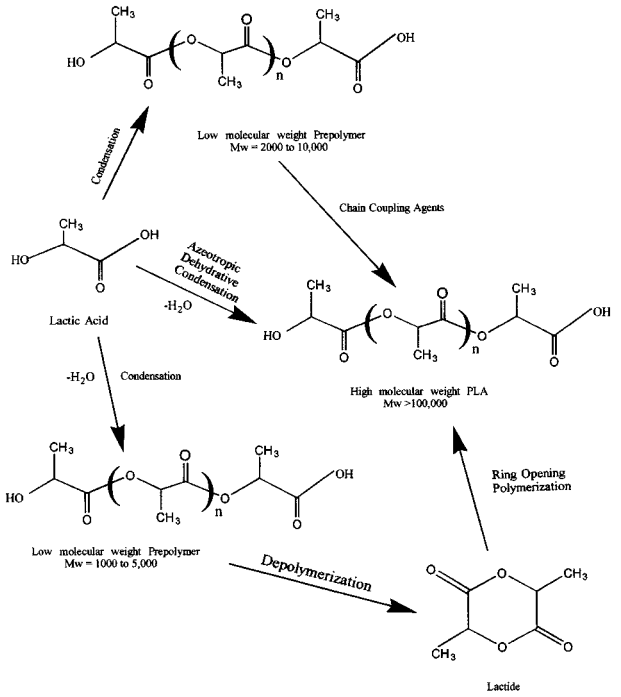

Fig. 1. Synthesis methods for high-molecular-weight PLA [1, 29].

maintain cell growth and production, various methods of neutralization or extraction of the produced acid have been developed. The major method of separation consists of adding calcium hydroxide or calcium carbonate to neutralize the fermentation acid and give soluble calcium lactate solutions. This calcium lactate broth is filtered to remove the cell biomass and other insolubles, then evaporated, recrystalllized, and acidified with sulfuric acid to yield the crude lactic acid. The insoluble calcium sulfate (gypsum) is filtered off and discarded, with up to 1 ton of gypsum per ton of lactic acid produced. Typically, acid for polymer, pharmaceuticals, or food derivatives requires further purification to remove byproduct proteins and carbohydrates. Higher purity is obtained by distillation of the acid as the methyl or ethyl ester, followed by hydrolysis back to the acid [6–9].

The synthesis of lactic acid into high-molecular-weight PLA can follow two different routes of polymerization, as depicted in Fig. 1. Lactic acid is condensation polymerized to yield a low-molecular-weight, brittle, glassy polymer, which, for the most part, is unusable for any applications unless external coupling agents are used to increase the molecular weight of the polymer. The molecular weight of this condensation polymer is low due to the viscous polymer melt, the presence of water, impurities, the statistical absence (low concentration) of reactive end-groups, and the "back-biting" equilibrium reaction that forms the six-member lactide ring. The second route of producing PLA is to collect, purify, and ring-open polymerize (ROP) lactide to yield high-weight-average molecular weight ($M_w > 100{,}000$) PLA. The lactide method was the only method of producing pure, high-molecular-weight PLA until Mitsui Toatsu Chemicals recently commercialized a process wherein lactic acid and catalyst are azeotropically dehydrated in a refluxing, high-boiling, aprotic solvent under reduced pressures to obtain PLA with weight-average molecular weights greater than 300,000 [10–13].

Figure 1 depicts the known routes to high-molecular-weight PLA: condensation/coupling, azeotropic dehydrative condensation, or ring-opening polymerization of lactide. The condensation polymerization is the least-expensive route, but it is difficult in a solvent-free system to obtain high molecular weights, and therefore the use of coupling agents or esterification-promoting adjuvants is required, adding cost and complexity [14–28]. The self-condensation of lactic acid results in a low-molecular-weight product with an equimolar concentration of hydroxyl and carboxyl end-groups. To increase the molecular weight, chain-coupling agents must be added, and these will preferentially react with either the hydroxyl or carboxyl group, which leads to different kinetic reaction rates of coupling. The condensed PLA can be modified to produce either all hydroxyl or all carboxyl groups. Hydroxyl-terminated PLA can be synthesized by the condensation of lactic acid in the presence of a small amount of multifunctional hydroxyl compounds such as 2-butene-1,4-diol, glycerol, or 1,4-butanediol, which leads to preferential hydroxyl end-groups, or by the postcondensation reaction of a monofunctional epoxide such as butyl glycidyl ether with the carboxylic acid to convert it to a hydroxyl group [23]. This same concept can be used to synthesize an all-carboxyl-terminated PLA by the condensation reaction in the presence of multifunctional carboxylic acids such as maleic, succinic, adipic, or itaconic acid, leading to a carboxyl functional polymer [19–21]. The PLA can also be postreacted with acid anhydrides such as maleic or succinic to convert the hydroxyl to a carboxylic end-group [21].

Various esterification-promoting adjuvents and chain-extending agents have been reported that can be used to increase the molecular weight of the PLA condensation products [14]. Some examples of the esterification-promoting adjuvents are bis(trichloromethyl) carbonate, dicyclohexylcarbodiimide, and carbonyl diimidazole. These adjuvents produce reaction byproducts that must be either neutralized or removed. Bis(trichloromethyl) carbonate creates hydrochloric acid, which can degrade the polymer, or dicyclohexylcarbodiimide forms unreactive and insoluble dicyclohexylurea, which can be filtered

out during the final purification steps. The advantages of esterification-promoting adjuvents are that the final product is highly purified—free from residual metals, catalyst, and low-molecular-weight oligomers. The disadvantages are higher costs due to the increased number of reaction steps, the use of dangerous or flammable solvents, inability to form copolymers containing different functional groups, and the additional purification and separation steps of nonrecoverable byproducts [1].

The use of chain-extending agents overcomes many of the disadvantages associated with esterification-promoting adjuvents. Reactions involving chain-extending agents are more economically feasible, as they can be done in the melt with lower amounts of chain-extending agents required and separate chain-extending steps aren't needed. Improved mechanical properties associated with the chain-extending agent are also found, and the flexibility to manufacture copolymers with different functional groups is greatly expanded. The disadvantages are that the final polymer may still contain unreacted chain-extending agents, residual metal, or polymer impurities, or the extending agents are not biodegradable or bioabsorbable [1]. Some examples of chain-extending agents are isocyanates, acid chlorides, anhydrides, epoxides, thiirane, and oxazoline. The disadvantages of using isocyanates as chain extenders are the toxicity and sensitivity effects associated with the isocyanate monomers and their subsequent toxic amine hydrolysis products [1].

The azeotropic condensation polymerization is a method to obtain high-molecular-weight polymer without the use of chain extenders or adjuvents. Copolymers using various diacids, diols, or hydroxy-acids are possible, with the use of solvents and residual catalyst the main drawbacks. A general procedure for this route consists of reduced pressure distillation of lactic acid for 2 to 3 hours at 130°C to remove the majority of the condensation water. Catalyst and diphenyl ether are added; then a tube packed with 3-Å molecular sieves is attached to the reaction vessel. The refluxing solvent is returned to the vessel by way of the molecular sieves for an additional 30–40 hours at 130°C. The polymer can then be isolated as is or dissolved and precipitated for further purification [10–13, 30, 31].

This polymerization technique yields high-molecular-weight polymers, but with considerable catalyst impurities due to the high levels needed for acceptable reaction rates. This residual catalyst can cause many problems during further processing, such as unwanted degradation, uncontrolled or unreproducible hydrolysis rates, or, in the case of medical applications, catalyst toxicity and differing slow-release properties. The catalyst can be deactivated by the addition of phosphoric or pyrophosphoric acid, and preferably two equivalents of acid to divalent tin catalyst are used. This provides a polymer with improved weathering resistance and heat and storage stability. The catalyst can also be precipitated and filtered out by the addition of strong acids such as sulfuric acid. Catalyst levels can be reduced to 10 ppm or less [1, 32].

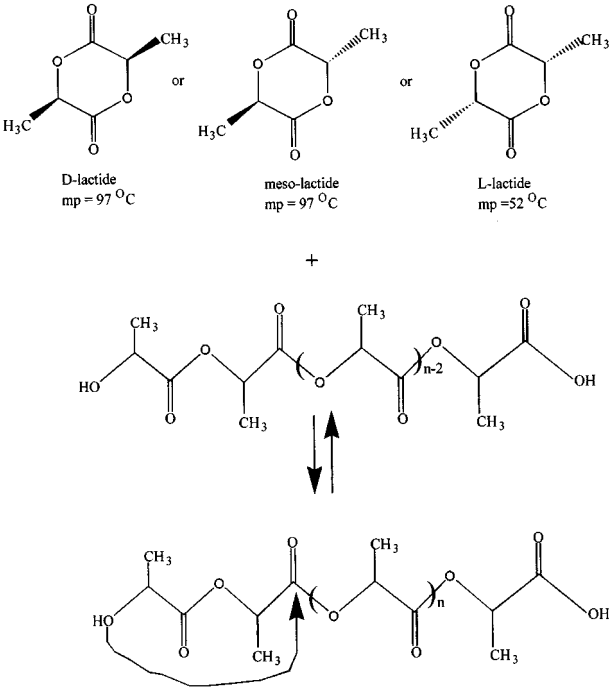

Fig. 2. Lactide ring formation.

The ring-opening polymerization of lactide was first demonstrated by Carothers in 1932 [33], but high molecular weights were not obtained until improved lactide purification techniques were developed by DuPont in 1954 [34]. Lactide is obtained by the depolymerization of low-molecular-weight PLA under reduced pressure to give a mixture of L-lactide, D-lactide, or *meso*-lactide. The different percentages of the lactide isomers formed depends on the lactic acid isomer feedstock, temperature, and catalyst [1]. Figure 2 demonstrates the synthesis of PLA from the lactide ring. The D-lactide and L-lactide enantiomers can form a 1:1 racemic stereocomplex (D,L-lactide), which melts at 126–127°C [1, 29].

Poly(lactic acid) can undergo cationic ring-opening polymerization. It has been found that trifluoromethanesulfonic acid (triflic acid) and methyl trifluoromethanesulfonic acid (methyl triflate) are the only cationic initiators to polymerize lactide [35–37]. The polymerization proceeds via triflate ester end-groups instead of free carbenium ions, which yields, at low temperatures (<100°C), an optically active polymer without racemization. The chain growth proceeds by cleavage of the alkyl-

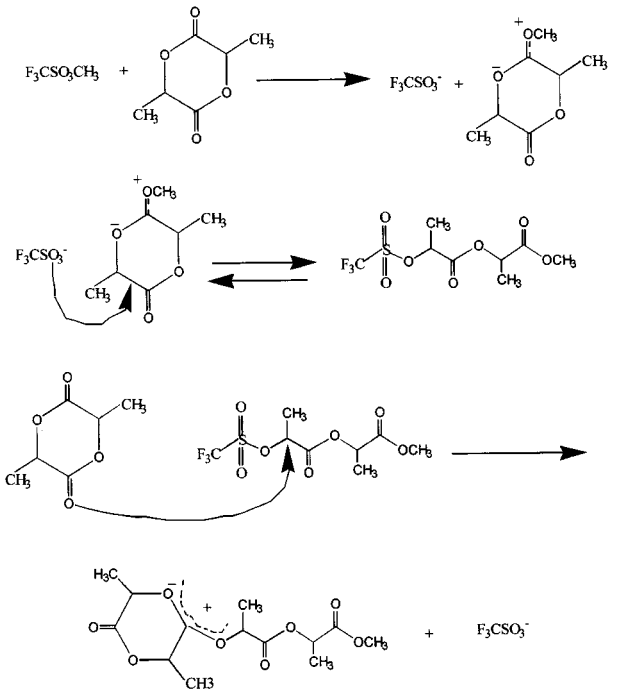

Fig. 3. Cationic ring-opening polymerization mechanism for PLA.

oxygen bond. The propagation mechanism begins with the positively charged lactide ring being cleaved at the alkyl-oxygen bond by an S_N2 attack by the triflate anion. The triflate end-group reacts with a second molecule of lactide again in an S_N2 fashion to yield a positively charged lactide that is opened. Then the triflate anion again opens the charged lactide, and polymerization proceeds [38]. The cationic polymerization mechanism is shown in Fig. 3 [1].

Anionic lactide polymerizations proceed by the nucleophilic reaction of the anion with the carbonyl and the subsequent acyl-oxygen cleavage. This produces an alkoxide end-group, which continues to propagate. The anionic polymerization mechanism is depicted in Fig. 4 [1]. Jedlinski *et al.* [39, 40] has shown that the use of primary alkoxides such as potassium methoxide can yield well-defined polymers with negligible racemization, termination, or transesterification. Racemization of less than 5% was seen, starting with 99.9% pure L-lactide [39, 40].

An extensive study of various anionic initiators for lactide polymerization was conducted. Kricheldorf *et al.*

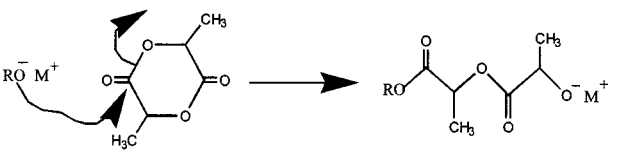

Fig. 4. Anionic ring-opening polymerization mechanism for PLA.

[41–43] found that initiators of higher nucleophilicity are needed to initiate the lactide. Weaker bases, such as potassium benzoate, potassium phenoxide, or zinc stearate, do not initiate at low temperatures, but will initiate at high temperatures (120°C). The high-temperature initiations occur in bulk but with considerable racemization and other side reactions, which hinder propagation [41–44]. Initiators such as *n-*, *sec-*, or *tert*-butyl lithium and potassium *tert*-butoxide rapidly initiate the polymerization at low temperatures, but are plagued by side reactions, such as deprotonation of the lactide monomer [45–47]. This deprotonation causes inconsistent polymerization, racemization, and, when done by the active chain end, termination, which thereby limits the molecular weights. Sipos *et al.* [48] reported that the use of 18-crown-6 ether complexes will yield higher molecular weights with narrow distributions, (PDI = 1.1–1.2), but they slow the rate and give lower overall conversions. There are toxicity concerns with the use of lithium initiators, whereas the use of potassium or sodium metal ions yields polymers that are less toxic and are considered biocompatible [1].

The anionic and cationic initiations as described above are usually done in solvent systems and, due to their high reactivities, are susceptible to racemization, transesterification, and especially impurity levels. For practical, large-scale commercial use, it is preferable to do bulk melt polymerizations that use lower levels of nontoxic catalysts and are not plagued by these previous problems. The use of less-reactive metal carboxylates, oxides, and alkoxides has been extensively studied to correct these problems. It has been found that high-molecular-weight PLA is easily polymerized in the presence of tin, zinc, aluminum, and other heavy metal catalysts, with tin(II) and zinc yielding the purest polymers. These catalysts are favored because of their covalent metal-oxygen bonds and free *p* or *d* orbitals [41, 49].

Kricheldorf and Serra [93] screened 24 different oxides, carbonates, and carboxylates in the bulk polymerization of lactide at 120, 150, and 180°C [43]. It was found that the most effective catalysts with respect to yield, molecular weight, and racemization were tin(II) oxide or octoate, lead(II) oxide, antimony octoate, and bismuth octoate. The best results were obtained with tin oxide and octoate at 120–150°C with conversions >90% and less than 1% racemization. Few carbonates gave acceptable polymerizations, and all had considerable racemization. The alkali metal carboxylates, such as sodium and calcium, were similar to the carbonates [40].

Previous research has led to the wide use of tin compounds, namely tin(II) bis-2-ethylhexanoic acid (tin or stannous octoate) as a catalyst in PLA synthesis. This

is mainly due to its solubility in many lactones, low toxicity, FDA approval, high catalytic activity, and ability to give high-molecular-weight polymers with low racemization [36, 50, 51].

The mechanism and polymerization variables of the tin octoate polymerization has been studied by various groups, but still considerable debate about the true mechanism remains. The effect of certain variables on the tin octoate- and zinc-catalyzed polymerization was studied. It was found that the yield and transesterification is affected, in order, by polymerization temperature > monomer-to-catalyst ratio > polymerization time > type of catalyst (Sn or Zn) > monomer degassing time. The interaction of time and temperature, as would be expected, was very significant since this leads to degradation reactions that will limit molecular weight and affect the reaction rate [52, 53]. It has been shown that the molecular weight is directly controlled by the amount of hydroxyl impurities and is independent of carboxylic acid impurities and catalyst concentration [54–62].

The polymerization kinetics have been studied and been found to be first-order in monomer and catalyst concentration [37]. The thermodynamics of polymerization of D,L-lactide and its polymer have been estimated by using adiabatic and isothermal calorimetry to measure the heat capacities and enthalpies of combustion. The calculated enthalpies and entropies of polymerization were found to be $\Delta H_p = -27.0$ kJ/mol and $\Delta S_p = -13.0$ J/mol-°K at 400°K [63, 64].

Witzke [62] developed a reversible kinetic model for the homopolymerization of L-lactide when catalyzed by tin octoate in bulk. The kinetic experiments were performed over a wide range of conversions, catalyst concentrations (1000–80,000:1 monomer-to-catalyst molar ratio), and temperatures, (130–220°C) and were used to calculate the thermodynamics. The following parameters were calculated: $E_a = 70.9 \pm 1.5$ kJ/mol, $\Delta H_p = -23.3 \pm 1.5$ kJ/mol and $\Delta S_p = -22.0 \pm 3.2$ J/mol-°K, and a $T_{ceiling} = 786 \pm 87$°C [1]. A model for monomer concentration or conversion as a function of time was then derived. It is as follows [62]:

$$M(t) = M_{eq} + (M_0 - M_{eq})e^{(-K_p It)} \quad (1)$$

$$X_{mon}(t) = (1 - M_{eq}/M_0)(1 - e^{(-K_p It)}) \quad (2)$$

$$K_p = 86.0e^{(-E_a/R(1/T - 0.00223))} \quad (3)$$

$$M_{eq} = e^{(\Delta H_p/RT - \Delta S_p R)} \quad (4)$$

where

$M(t)$ = monomer concentration at time (t)
M_{eq} = equilibrium monomer concentration
M_0 = Initial monomer concentration
K_p = propagation rate constant in 1/cat. mole%-hr
I = catalyst concentration in mole %
t = time in hours
X_{mon} = monomer to polymer conversion at time (t)
E_a = energy of activation
R = gas constant
T = polymerization temperature in Kelvin
ΔH = enthalpy of polymerization
ΔS = entropy of polymerization

The rates of chain growth vary greatly in a polymerization catalyzed with tin octoate and depend not only on impurities but also on the formation of crystalline phases during polymerization. It has been shown by Witzke and Nijenhuis [60, 62] that the apparent rate of propagation will increase and the apparent equilibrium monomer concentration will decrease when crystalline polymer domains form during polymerization. They had shown that when L-lactide is polymerized below the polymer crystalline melting temperature, crystalline domains form that exclude both monomer and catalyst. This constant enrichment of the amorphous phase leads to increased concentrations of catalyst, which lead to higher polymerization rates. The apparent equilibrium monomer concentration is reduced in the total system due to lower percentage of amorphous (which holds the equilibrium monomer concentration and catalyst) to crystalline phases. The apparent equilibrium monomer concentration is in direct proportion to the degree or percent of amorphous phase in the polymer [62].

The addition of hydroxylic or carboxylic impurities has also been shown to greatly affect the polymerization rate. The addition of lactic impurities (i.e., water, lactic acid) does not significantly affect the polymerization rate, only the final molecular weight [58, 62]. This is theoretically due to the presence of both hydroxyl and carboxyl groups. The addition of free carboxylic acids, however, has an inhibitory effect on the polymerization rate but does not affect the final molecular weight. This may be due to the free acids, which preferentially do not react with the lactide but complex with the catalyst and lower its catalytic activity. Hydroxylic impurities have the opposite effect. They increase the rate of polymerization in proportion to their concentration and also directly control the final molecular weight. This would point to the hydroxylic compounds interacting with both the catalyst and the lactide. Van Der Weij [65] has shown that tin octoate will hydrolyze to give catalytically more active hydroxide or alkoxide derivatives, as shown in Fig. 5 [65, 66]. Both residual water and alcoholic coinitiators

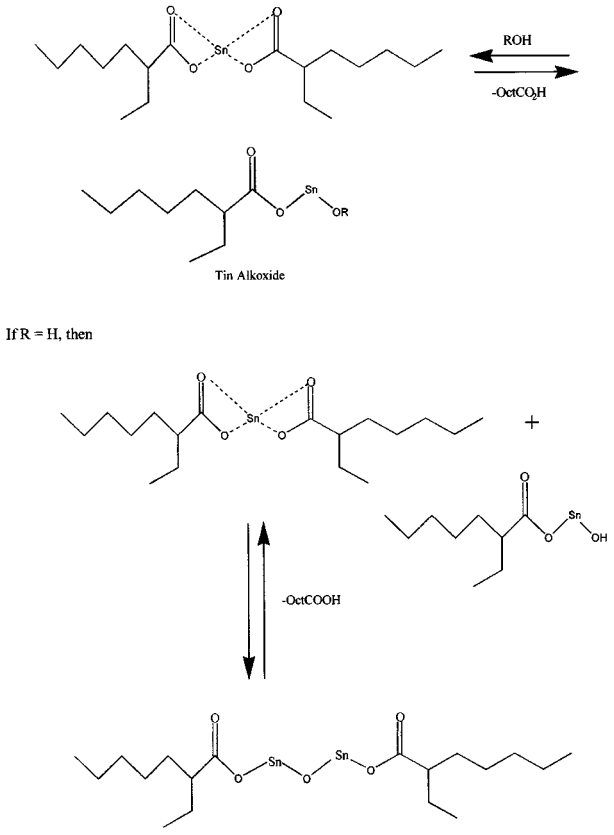

Fig. 5. Tin octoate reactions

used can react with the tin octoate to produce these more-active catalysts [1].

Other tin compounds have shown promise, including tetraphenyl tin, tin(II) and tin (IV) halogenides, and tin(II) acetylacetonoate [36, 50, 59, 60]. Ten-membered dimeric cyclic initiators based on dibutyl tin oxide were prepared and reacted with 1,2-ethanediol or 1,2-mercaptoethane. It was found that only the Sn-O bond containing the catalysts (not Sn-S) will catalyze the polymerization [67]. These cyclic catalysts, due to the coordination/insertion mechanism, form high-molecular-weight PLA macrocycles with little racemization when polymerized in bulk at 120°C. Distannoxane complexes have also shown high efficiencies in copolymerization of various lactones and lactide [68]. The use of solid heterogenous tin catalysts has recently been reported. The polymerization of lactide with a tin-substituted mesoporous silica molecular sieve gave polymers of higher molecular weights, higher conversions, and narrower molecular weight distributions when compared to SnO_2 [69].

Aluminum alkoxides are another catalyst system that proceeds through the coordination/insertion mechanism, and are reported to give controllable molecular weights with narrow distributions [70, 71]. Jedlinski [72] found that $ZnEt_2$ and its complex with $Al(OiPr)_3$ gave rapid polymerization with low transesterification when D,L-lactide was polymerized in bulk at 150°C. Similar results were obtained using $Al(OiPr)_3$ in the bulk of 100°C, and using proton NMR it was found that all chains contained isopropoxy ester end-groups and molecular weights corresponding to the number of alkoxide groups [73]. These results demonstrate that the aluminum alkoxide initiates the lactide polymerization by an acyl-oxygen cleavage and that all the ligands are active initiating species. It was found that there was no transesterification at temperatures less than 150°C, which yields polymers with narrow molecular weight distribution [73]. Dubois *et al.* [74, 75] studied the kinetics and the mechanism of the aluminum alkoxide polymerization in solution. It was found that after an initial induction period, the polymerization is first-order in both monomer and initiator. This "living" polymerization is characterized by the linear dependence of the number average molecular weight on the monomer-to-initiator molar ratio and conversion. This yields polymers with a polydispersity index of 1.1 to 1.4 and no intra- or intermolecular side reactions. For $Al(OiPr)_3$ in toluene at 70°C, there are three active sites per aluminum molecule, which is in contrast to other lactone polymerizations where the number of active sites is less due to catalyst aggregate formation [74, 75]. The mechanism (Fig. 6) involves the insertion of the lactide into the aluminum-alkoxide bond with lactide acyl-oxygen cleavage [76].

A new series of lactide polymerization catalysts has been developed that gives rapid living polymerizations with low-molecular-weight distributions [77–82]. Scientists at DuPont have researched rare earth compounds based on lanthanum and yttrium as initiators for both solvent and bulk lactone polymerizations. They report room-temperature lactide polymerizations that achieve full conversion after 15 minutes using a 417:1 molar catalyst ratio (lactide:catalyst) and a polydispersity of 1.15 [77–79]. Some examples of rare earth catalysts that were investigated were yttrium tris(*N*,*N*-dimethylaminoethoxide), yttrium tris(methyllactate), samarium tris(*N*,*N*-dimethyl-aminoethoxide), and lanthanum tris(2,2,6,6-tetramethylheptanedionate) [77–82].

EXPERIMENTAL RESULTS AND DISCUSSION OF POLY(LACTIC ACID)

The mechanical properties and crystallization behavior of PLA is very dependent on the molecular weight and stereochemical makeup of the backbone. This stereo-

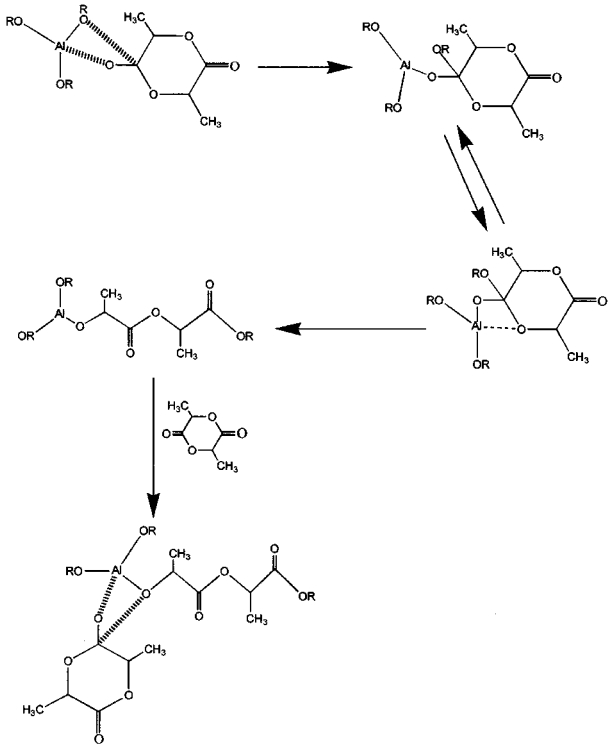

Fig. 6. Aluminum alkoxide polymerization mechanism [76].

chemical makeup is very easily controlled by the polymerization with D-lactide, L-lactide, D,L-lactide, or *meso*-lactide, to form random or block stereocopolymers, while the molecular weight is directly controlled by the addition of hydroxylic compounds (i.e., lactic acid, water, alcohols) [1]. The ability to control the stereochemical architecture allows precise control over the speed and degree of crystallinity, the mechanical properties, and the processing temperatures of the material. The hydrolytic degradation of the polymer matrix is affected by the amount of crystallinity in the samples. It has been shown that highly crystalline PLA will take months, sometimes years, to hydrolyze fully to lactic acid, whereas an amorphous sample is degraded in weeks. This is due to the impermeability of the crystalline region [9, 83].

Pure poly(D-Lactide) or poly(L-Lactide) has an equilibrium crystalline melting point of 207°C [56, 57, 84, 85] but typical melting points are in the 170°C–180°C range. This is due to small and imperfect crystallites, slight racemization, and impurities. It has also been observed that a 1:1 mixture of pure poly(L-lactide) with pure poly(D-lactide) will yield an insoluble gel formed by the stereocomplexation (racemic crystallite) of the two polymers during crystallization or polymerization. This pure stereocomplex has a melting point of 230°C and mechanical properties greater than either pure polymer

Table I. Calculated and Observed *d* Spacings (Å) of the β Structure of Poly(L-Lactide) with the Orthorhombic Unit Cell; $a = 10.3$, $b = 18.2$, and $c = 9.0$

h,k,l	$d_{h,k,l}$ (calc.)	$d_{h,k,l}$ (observed)	Intensity
200	5.16	5.17	vs
330	2.99	3.00	m
111	6.35	6.20	w
112	4.02	3.98	m
222	3.18	3.17	m
240	3.41	3.40	m
221	4.02	4.02	s

[86–93]. Using lower-molecular-weight PLA, it has been reported that ultimate tensile strengths were 50 MPa for the 1:1 stereocomplex versus 31 MPa for pure L-PLA [86, 87]. Variations such as block and star copolymers of D- and L-lactide show this same stereocomplexation [1].

The enthalpy of melting ΔH_m) for a pure crystal (100% crystallinity) was calculated through extrapolation to be 93.7 joules/gram, with practical ΔH_m in the 40–50 joules/gram range, yielding polymers with 37–47% crystallinity [94–96]. Runt et al. [97] and Nijenhuis et al. [59] have reported this value to be 100 joules/gram for slowly polymerized, highly crystalline poly(L-lactide). The extent of crystallinity, and therefore the melting point, can easily be varied, and greatly depends on the annealing or polymerization conditions and amount of *meso*-, D-, or L-lactide [1].

Marega et al. [98] showed that the α-form of poly(L-lactic acid) has a pseudo-orthorhombic unit cell containing 2 10_3 (10 Å rise/3 monomeric units) polymeric helices. The unit cell dimensions are as follows: $a = 10.7$ Å, $b = 6.126$ Å, and $c = 28.939$ Å, with the diameter distribution of the crystallites ranging fom 390 to 440 Å. Earlier, Hoogsteen et al. [99] showed that the β-form of poly(L-lactic acid) has an orthorhombic unit cell (containing 6 chains) containing a 3_1 (3 Å rise/1 monomeric unit) polymeric helix. The unit cell dimensions are as follows: $a = 10.31$ Å, $b = 18.21$ Å, and $c = 9.0$ Å [99]. It has been reported that the α-structure has a melting point of 185°C, versus 175°C for the β-structure, suggesting that the α-structure is more stable than the β-structure [99]. Representative tables of *d*-spacings of the β-structure of PLLA, discrete energy minima of PLLA chains, and standard bond lengths and angles used in conformational energy calculations are presented in Tables I to III [99].

Kalb and Pennings [85] had grown PLLA crystals in various solvents. Growing PLLA crystals in toluene and *p*-xylene (0.08 wt%) yielded large lamellar single crystals. For the crystals grown in toluene at 55°C, the

Table II. Discrete Energy Minima for PLLA Chains according to the Conformational Energy Calculations of Flory

	Ψ	Φ, degree	E, kcal/mol	State
I	130	110	0.08	$g^+_\Psi\ g^+_\Phi$
II	130	20	1.40	$g^+_\Psi\ t_\Phi$
III	−20	110	0	$t_\Psi\ g^+_\Phi$
IV	−20	20	1.52	$t_\Psi\ t_\Phi$

t = trans; g = gauche

lamellae were lozenge shaped and had a thickness of 10 nm. The growth of the crystals occurred along four planes. For single crystals prepared from *p*-xylene at 90°C, the thickess of the lamellae was 12 nm, and the growth of the crystals occurred along six planes. Electron diffraction patterns on the single crystals suggested that the crystal lattice spacing was 5.17 ± 0.08 Å for all reflections in the spot pattern. The electron diffraction results suggest that the molecular chains were oriented in the direction orthogonal to the basal plane of the crystal and that the unit cell is hexagonal, having dimensions of $a = b =$ 5.9 Å, $\alpha = \beta = 90°$, and $\gamma = 120°$. The magnitude of *c* could not be determined.

In addition to the dependence on the molecular weight and the L-concentration, the rate and extent of crystallization also depend on the presence or absence of nucleating agents as well as the time-at-temperature above T_g [100]. Crystallization of the amorphous, but thermally crystallizable, PLA copolymers (various L- to D-content) by annealing could be initiated at temperatures between 75°C and the melting point. Annealing crystallizable PLA copolymers to induce crystallinity often produced two melting peaks [100]. This is what was observed at the USDA-NCAUR (Peoria, IL) with PDLLA in injection-molded starch/PDLLA/adipic PHEE blends. Lack of a crystallization exotherm suggested that the PDLLA in the blend reached the maximum crystallization rate possible, Bigg [100] found that annealing at 3-mm-thick PLA tensile bar beyond 5 minutes at 110°C produced no observable increase in the degree of crystallinity achieved. Annealing for 1 minute or less didn't allow the sample enough time to heat up to the temperature range required for annealing [100]. Annealing at higher temperatures, (i.e., 135°C) didn't produce complete crystallization. Annealing at temperatures close to the melting point produced only those crystals with the highest melting point. Longer annealing times are required to produce the more perfect, higher-melting crystals. This is a result of first melting the less perfect, lower-melting crystals and then reforming them into higher-melting, more perfect crystals. This change in crystallization process from rapidly forming, lower-melting crystals to more slowly reforming, higher-melting crystals occurred gradually as the annealing temperature progressed from 100°C to 140°C [100]. For starch/PDLLA/adipic PHEE blends, annealing for less than 5 minutes didn't allow the sample enough time to heat up to the required annealing temperature. As the annealing time increased, so did the crystalllinity of the PDLLA in the starch/PDLLA/adipic PHEE blends.

Table III. Standard Bond Lengths and Bond Angles Used in the Conformational Energy Calculations

Bond	Length, Å	Bond	Angle, degree
O(ester)—C_α	1.46	O_{ester}—C_α—C_c	109.5
C_α—C(carbonyl)	1.53	C_α—C_{ester}—O_{ester}	110
C(carbonyl)—O(ester)	1.31	C_c—O_{ester}—C_α	118
C(carbonyl)—O(carbonyl)	1.19	O_c—C_c—O_{ester}	125
C_α—C_β	1.52	O_{ester}—C_α—H_α	109.5
C_α—H_α	1.05	O_{ester}—C_α—C_β	109.5
C_β—H_β	1.05	C_α—C_β—H_β	109.5

Bigg [100] also investigated the effects of molecular weight and nucleating agents on the crystallinity of PDLLA. A sample of 400,000 g/mole showed no crystallization exotherm or melting endotherm. This sample would be very difficult to process anyway. Samples of less than 300,000 g/mole developed 30–50% crystallinity. Addition of 1% calcium lactate, by weight, increased the rate of crystallization of a 90/10 L/D isomeric ratio in PLA to the point where no crystallization exotherm was observed during heating of a polymer sample that had been quenched from the melt during injection molding. Again, even the nucleated polymer could be quenched rapidly enough to inhibit crystal formation [100].

Poly(lactid acid) is a slower-crystallizing material, similar to poly(ethylene terephthalate). The fastest rates of crystallization for pure PLA are found in the temperature range of 110–130°C, which yields spherulitic crystalline morphology [95, 98, 101–106]. A measured spherulitic growth rate has been determined, at 125°C, to be 4.0, 2.0, and 0.8 μm/min for pure PLLA, and 3.0%, and 6% for *meso*-containing polymer, respectively [105]. Kolstad [103] studied the crystallization kinetics of poly(L-co-*meso*-lactide) and found that the crystallization half time increased approximately 40% for every 1 wt% increase in the *meso*-lactide. He also found that the addition of 6%, by weight, of talc as a nucleating agent increased the nucleation density greatly, reducing the crystallization half times. The addition of talc reduced the 110°C half time from 180 sec to 25 sec for pure poly(L-lactide) and from 420 to 60 sec for a 3% *meso*-

Table IV. Nucleation Parameters from Isothermal and Nonisothermal Kinetic Analysis for PLLA

Parameter	Isothermal	Nonisothermal
K_g	2.44×10^5	2.69×10^5
$\sigma\,\sigma e \times 10^6$ (J^2/m^4)	753.0	830.4
σ	12.03×10^{-3} J/m^2	13.6×10^{-3} J/m^2

containing polymer. He also found that the polymer lost its ability to crystallize when the minor isomer content exceeded 15% [103], which is in good agreement with Fischer [94].

Kishore and Vasanthakumari determined the nucleation parameters for poly(L-lactic acid) crystallization from nonisothermal thermal analysis experiments using DSC [107] (Table IV). The values of the nucleation constant, K_g; lateral surface energy, σ; fold surface energy, σe; layer thickness of the crystal, b; and heat of fusion/unit volume, ΔH_f were determined for poly(L-lactic acid). The following equation was used in conjunction with Table IV:

$$K_g = \frac{4b\ \sigma\ \sigma e T_m}{\Delta H_f\, k} \qquad k = \text{Boltzmann constant} \quad (5)$$

The following values were input into the equation above to obtain the aforementioned values:

$$T_m = 480°\text{K}\ (207°\text{C})$$

$$T_g = 328°\text{K}\ (55°\text{C})$$

$$\Delta H_f = 11.11 \times 10^8\ \text{erg/cm}^3\ (111.083 \times 10^6\ \text{J/m}^2)$$

$$b = 5.17 \times 10^{-8}\ \text{cm}$$

$$\sigma e = 60.89\ \text{erg/cm}^2\ (6.089 \times 10^{-4}\ \text{J/m}^2)$$

The peak crystallization temperature was 125°C [107].

Kalb and Pennings [85] carried out some isothermal crystallization experiments of PLLA using optical microscopy. They used a temperature of 120°C. The growth of the spherulites started after 1 minute, and the growth rate was 10.6 μm/min. They noted the existence of negatively birefringent spherulites. Since fibers of PLLA have a higher refractive index in the axis direction, the negative birefringence present appears to be due to the fact that molecular chains are oriented in the direction orthogonal to the radius of the spherulites, which has been found to be a general feature for spherulites. After carrying out crystallization experiments using the DSC, they suggested that poly(L-lactic acid) crystallinity might not exceed 60%.

Kalb and Pennings [85] dissolved PLLA crystals in *p*-xylene and studied their dissolution temperature as a function of crystallization temperature, T_c, using differential scanning calorimetry. They arrived at an equilibrium dissolution temperature, T_d°, of 126.5°C. This is of relevance to fiber-forming processes. They had used the following equation to calculate the surface energy at the fold surface:

$$\sigma e = \frac{L\ \Delta H_f\, \rho c (T_d^\circ - T_c)}{2T_d^\circ} \quad (6)$$

where

$$L = 12\ \text{nm at}\ T_c = 90°\text{C}$$

$$\rho c = 1290\ \text{kg/m}^3$$

$$\text{for}\ T_d^\circ = 126.5°\text{C, then}\ \sigma e = 75 \times 10^{-3}\ \text{J/m}^2$$

$$\Delta H_f = 6200\ \text{J/mol}$$

Vasanthakumari and Pennings [84] also performed crystallization kinetics studies on poly(L-lactic acid). They mentioned the Hoffman–Weeks equation that relates T_m to T_c). The equation is as follows:

$$T_m = T_m^\circ\ (1 - 1/2\beta) + T_d/2\beta$$

where β is a constant depending on the edge free-surface energy.

Heating rate (°C/min)	β
4	1.2
5	1.3
8	1.4

The Hoffman–Weeks equation can be alternatively written as [97]

$$\mathrm{T}_m = \mathrm{T}_m^\circ \left[1 - \frac{2\ \sigma e}{\Delta H_f^\circ\ (lc)} \right] \quad (7)$$

where *lc* is the lamella thickness.

Table V summarizes the work of Vasanthakumari and Pennings [84].

Urbanovici *et al.* [108] obtained isothermal DSC crystallization data for poly(lactic acid). They chose six temperatures (ranging from 90 to 130°C) for the isothermal crystallization experiments. For each isothermal crystallization temperature, they presented the Avrami parameters as well as the enthalpy of crystallization. The Avrami equation can be stated as follows:

$$-\ln(1 - \alpha) = Zt^n = (kt)^n; \qquad k = Z^{-n} \quad (8)$$

Avrami equation

Table V. Crystallization Kinetics Data for Poly(Lactic Acid)

Sample number	Mv $\times 10^{-5}$	T_g (°K)	log G_0	G_0 (μm/min)	$K_g \times 10^{-5}$	$\sigma\,\sigma e \times 10^6$ (J^2/m^4)
A	6.9	333	7.19	1.56×10^7	2.34	722
B	3.5	331	7.21	1.63×10^7	2.29	706
C	2.6	330	7.38	2.40×10^7	2.37	732
D	1.5	328	7.53	3.38×10^7	2.44	753

$$\alpha = 1 - \exp[-(kt)^n] \tag{9}$$

$$d\alpha/dt = nk(1 - \alpha)[-\ln(1 - \alpha)]^{(n-1)/n} \tag{10}$$

$d^2\alpha/dt^2 = 0$, then $\alpha_{max} = 1 - \exp[(1 - n)/n]$

and $t_{max} = (1/k)[(n - 1)/n]^{-1/n}$ (11)

where

α = degree of crystallization (i.e., fraction of crystalline volume developed at a given time, t)
Z = temperature-dependent rate constant
n = Avrami exponent
k = normalized rate constant

Runt *et al*. [97] presented crystallization kinetics data for copolymers of poly(L-lactide-co-*meso*-lactide). At a crystallization temperature of 117°C, a copolymer of 0.4% D-content crystallized 60 times faster than a copolymer of 6.6% D-content. At 135°C, the dependence of growth rate on *meso* concentration was much more significant. The ratio of growth rates of the 0.4% to 6.6% meso concentration was more than 340. This behavior is a manifestation of the reduction in equilibrium melting temperature with *meso* concentration. Runt suggested that the temperature where the maximum growth rate occurred shifted to a lower temperature with an increase in the D-isomer content. (T_{Gmax} = 129°C for a 0.4% D-isomer content to 120°C for a 6.6% D-isomer content). Table VI summarizes Runt's data [97].

Kolstad [103] also performed isothermal crystallization kinetics studies of poly(L-lactide-co-*meso*-lactide), similar to the work of Runt. He calculated the Avrami exponent, *n*, as well as the rate constant, *k*, and presented the data. He also presented data using Ultrafine talc 609 as a nucleating agent. His work was fairly comprehensive, and this publication should be investigated prior to any crystallization kinetics studies. A partial summary of Kolstad's data is given in Tables VII and VIII. The crystallization half time is the time required for the extent of crystallization, *x*, to reach 0.5.

Table VI. Mixed Isomer Crystallization Kinetics Data for Poly(Lactic Acid)

Sample	% *meso*-lactide	% D-isomer content	G_{max} (μm/min)
A	0	0.4	4.5
B	3	2.1	1.9
C	6	3.4	0.8
D	12	6.6	0.07

Lalla and Chugh [109] polymerized D,L-lactide using 2% (w/v) and 0.1% (w/v) zinc oxide and stannous chloride catalyst systems, respectively. They had characterized the physicochemical properties of the poly(lactic acid) synthesized by each of the aforementioned catalyst systems. The results are presented in Table IX [109]. The mechanical properties of poly(lactic acid) were studied. The results are listed in Table X. The wide variance in the oriented properties is due to the degree of orientation and stereochemical composition of various poly(lactic acid) samples. Table XI lists the effects of stereochemistry and crystallinity on the mechanical properties of amorphous L-PLA, annealed L-PLA, and amorphous D,L-PLA [1, 110]. The extent of crystallinity is not mentioned for the samples in Table 11. On annealing, the impact resistance increased due to the crosslinking effects of the crystalline domains, while the tensile strength increased, presumably due to the stereoregularity of the chain [1, 110]. Experimental results of the mechanical properties, obtained on two different grades of poly(lactic acid) supplied by Cargill, are presented in Table XII. The results were obtained at the USDA-ARS-NCAUR, Peoria, IL. The literature reports density values for poly(L-lactic acid) [112]. The density of amorphous PLLA is 1.248 g/ml. The density for crystalline PLLA is 1.290 g/ml.

Perego *et al.* [110] studied the effects of molecular weight and crystallinity on the mechanical properties of PLA by polymerizing pure L-lactide and D,L-lactide to create amorphous or semicrystallline polymers. They found that the glass transition temperature wasn't greatly affected by the stereochemical makeup or the range of molecular weights tested. Jamshidi et al. [3] found that PLA with a molecular weight of 22,000 g/mole has a T_g of 55°C which is only 4–5°C lower than that predicted for PLA of infinite molecular weight. The modulus and tensile strengths were greatest for PLA polymers with a

Table VII. Crystallization Half Time (Minutes) Data for Polylactide [103]

	0% *meso*		3% *meso*		6% *meso*	
Temperature (°C)	M_n = 101 K	M_n = 157 K	M_n = 88 K	M_n = 114 K	M_n = 58 K	M_n = 114 K
85	14.8		23.9			
90	7.0	11.4	11.0			
95	4.5		8.1			
100	3.8	4.8	9.4	11.4	27.8	
105	2.9					
110	1.9	4.0	6.0	10.8	19.7	44
115	3.5		6.9		22.2	
120	4.0	5.7	8.2	11.6		
125	5.1		11.5			
130	8.7	13.4				
135	22.9					

Table VIII. Crystallization Half Time (Minutes) Data for Polylactide with 6 wt% Talc [103]

Temperature (°C)	0 wt% *meso* (M_n = 123 K)	3 wt% *meso* (M_n = 105 K)	6 wt% *meso* (M_n = 122 K)	9 wt% *meso* (M_n = 81 K)
90	<1	2.0	5.7	8.8
100	<1	1.4	3.0	6.0
110	<1	<1	3.9	10.0
120	<1	2.1	14.7	≫15

Table IX. Comparison of Physicochemical Properties of Poly(Lactic Acid)

Properties	PLA(ZnO catalyst)	PLA($SnCl_2 \cdot H_2O$ catalyst)
Acid value	46	57
Hydroxyl value (%)	2.004	0.6234
Refractive index, n_D^{25}	1.456	1.439
Specific gravity, (gm/cc) 25°C	1.2604	1.2587
Ester value	740	726
Saponification value	786	783
Moisture content, (% w/w)	4.94	5.14
Softening range, (°C)	125–135°C	125–135°C

viscosity-average molecular weight above 55,000 g/mole [110]. The impact strength and Vicat softening temperature increased with crystallinity and molecular weight [110]. Injection molding PLA resulted in a molecular weight decrease of 14–40% [110]. Independent studies by DOW Chemical found that injection molding the general-purpose Cargill PDLLA didn't result in a molecular weight decrease, as determined by size exclusion chromatography/multi-angle light scattering(SEC-MALLS) (Table XIII). The molecular weights of the PDLLA prior to and after injection molding, as determined by SEC-MALLS, were statistically insignificant. Molecular weight studies, on the general-purpose, as well

Table X. Comparison of Physical Properties of High-Molecular-Weight PLA [5, 62, 111]

	Unoriented	Oriented[a]
Ultimate tensile strength(psi × 10^3, MPa)	6.9–7.7, 47.6–53.1	6.9–24, 47.6–166
Tensile yield strength (psi × 10^3, MPa)	6.6–8.9, 45.5–61.4	N/A
Tensile modulus (psi × 10^3, MPa)	500–580, 3447–4000	564–600, 3889–4137
Notched izod impact (ft-lb/in.)	0.3–0.4	N/A
Elongation at break (%)	3.1–5.8	15–160
Rockwell hardness	82–88	82–88
Specific gravity (g/cm^3)	1.25	1.25
Glass transition temperature (°C)	57–60	57–60

[a]Results depend on degree of orientation and isomer content.

Table XI. Effects of Stereochemistry and Crystalllinity on Mechanical Properties [1, 110]

		Annealed	
	L-PLA	L-PLA	D,L-PLA
Tensile strength (MPa)	59	66	44
Elongation at break (%)	7.0	4.0	5.4
Modulus of elasticity (MPa)	3750	4150	3900
Yield strength (MPa)	70	70	53
Flexural strength (MPa)	106	119	88
Unnotched izod impact (J/m)	195	350	150
Notched izod impact (J/m)	26	66	18
Rockwell hardness	88	88	76
Heat deflection temperature (°C)	55	61	50
Vicat penetration (°C)	59	165	52

as the injection-mold-grade, PDLLA, using dilute-solution viscosity, were performed at USDA-ARS-NCAUR in Peoria, Illinois. Extrusion and injection molding resulted in a molecular weight reduction (Tables XIII and XIV). The PDLLA was dissolved in tetrahydrofuran, and the viscosity studies were carried out at 31.15°C in a Ubbelohde viscometer. The Mark–Houwink equation that was used is as follows:

$$[\eta] = 5.50 \times 10^{-4}\ \mathrm{Mv}^{0.639} \qquad (12)$$

The viscosimetric studies revealed that there was a 21.85% and 41.00% molecular weight decrease when the PDLLA was injection molded and extruded, respectively (Table XIII). Tables XIII and XIV summarize the molecular weights of general-purpose and injection-mold-grade PDLLA prior to and after processing.

A possible explanation for the increase in the viscosity-average molecular weight of the injection-mold-grade PDLLA is that during processing (i.e., extrusion and injection molding) there was polymer chain entanglement, which led to an increase in the hydrodynamic volume, intrinsic viscosity, and, hence, the molecular weight of the polymer.

The refractive index increment, *dn*/*dc*, of poly(lactic acid) has been reported in the literature. This value is necessary in order to determine the weight-average molecular weight of a polymer by laser light scattering. The reported value is 0.148 ml/g at a wavelength of 632.8 nm in 1,1,1,3,3,3-hexafluoro-2-propanol (HFIP) [113]. Values of -0.0276 ± 0.0009 and -0.0280 ± 0.0006 ml/g, at a wavelength of 632.8 nm in benzene, were determined by a Wyatt DSP differential refractometer (Santa Barbara, CA) for general-purpose and injection-mold grades of PDLLA, respectively. These latter two values were determined at the USDA-ARS-NCAUR. The negative values are a result of benzene having a greater refractive index than poly(lactic acid). Because poly(lactic acid) has a similar refractive index to chloroform and tetrahydrofuran, the refractive index increments for poly(lactic acid) in these two solvents are too low to report.

Bigg [100] also mentioned the effect of temperature on the degradation of PLA. Poly(lactic acid) quickly loses

Table XII. Comparison of Physical Properties of Poly(D,L-Lactic Acid) Supplied by Cargill

Type of PDLLA	Percent of D-isomer	Ultimate tensile[a] strength (MPa)	Percent[a] elongation	Young's[a] modulus (MPa)	Specific gravity	Glass-Transition temp. (°C)[d]
General purpose	5%	67 ± 1.15	11.3 ± 0.40	914 ± 37.7	1.25[b]	55
Injection mold grade	3.6%	72.356 ± 0.832	11.346 ± 1.254	1279.907 ± 109.05	1.27[c]	55

[a] ASTM method D-638.
[b] MSDS.
[c] ASTM method D-792.
[d] DSC at 10°C per minute.

Table XIII. Effect of Processing on Molecular Weight of General-Purpose Cargill–Dow PDLLA (5% D-Isomer Content)

Process	Mol. wt. method	M_n (g/mol)		M_w (g/mol)
Before injection molding	SEC-MALLS	53,000		168,000
After injection molding	SEC-MALLS	54,500		173,000
Before injection molding	Dilute solution viscometry		M_v = 187,562	
After injection molding	Dilute solution viscometry		M_v = 146,571	
Before twin-screw extrusion	Dilute solution viscometry		M_v = 187,562	
After twin-screw extrusion	Dilute solution viscometry		M_v = 110,654	

Note: SEC/multi-angle laser light scattering used chloroform as solvent.

Table XIV. Effect of Processing on Molecular Weight of Injection-Mold-Grade Cargill–Dow PDLLA (3.6% D-Isomer Content)

Process	Mol. wt. method	M_n (g/mol)	M_w (g/mol)
Before injection molding	Gel permeation chromatography	98,000	203,000
Before injection molding	Dilute solution viscometry	M_v = 164,737	
After injection molding	Dilute solution viscometry	M_v = 195,333	
Before twin-screw extrusion	Dilute solution viscometry	M_v = 164,737	
After twin-screw extrusion	Dilute solution viscometry	M_v = 173,729	

Note: Gel permeation chromatography used a THF/methylene chloride mixture as a solvent.

its thermal stability when heated above its melting point. A significant level of molecular degradation occurred when PLA was held 10°C above its melting point (160°C) for a sustained period of time. Migliaresi et al. [114] had shown that thermal degradation was due to chain splitting and not hydrolysis [114]. They observed molecular weight reductions greater than 50% and concluded that large molecular weight reductions were unavoidable. Oxidation of PLA didn't occur to a measurable extent during thermal degradation.

The degradation process was complicated by the action of more than just molecular weight degradation. Another process-limiting phenomena associated with the upper limit of thermal processing was the development of color in the natural polymer when processed above 200°C. When the residual monomer level of the polymer dropped below 6% during extrusion at 190°C, color developed in the water-white polymer. Residence times were as little as 1 minute under a blanket of nitrogen. When the residual monomer level exceeded 6%, the polymer became water white, unless the extrusion temperature exceeded 200°C [100]. The L-PLA has a narrow window of processing, (12°C), whereas a 90/10 L- to D-copolymer has a much wider range of processing (40°C) due to its lower melting temperature.

Bigg [100] had shown tables, graphs, and DSC thermograms of the various PLA samples investigated. Some of the tables shown are T_g and T_m of PLA (Table XV), effect of temperature on the molecular weight of PLA (Table XVI), and the effect of processing conditions on the mechanical properties of PLA (Table XVII). Some of the graphs shown are dynamic modulus versus temperature, viscosity versus shear rate, and viscosity versus weight-average molecular weight of PLA.

Jamshidi et al. presented Fox–Flory plots [3] of PLLA and PDLLA. The Fox–Flory equation relates the glass-transition temperature, T_g, to the number-average molecular weight as follows:

$$T_g = T_g^{\infty} - K/M_n \tag{13}$$

where

$T_g^{\infty} = T_g$ at infinite molecular weight

K = a constant representing the excess free volume of the end-groups of the polymer chains Jamshidi [3] reported the values as follows:

T_g^{∞} = 58°C for PLLA and 57°C for PDLLA

$K = 5.50 \times 10^4$ for PLLA and 7.30×10^4 for PDLLA

For PLLA Jamshidi [3] presented the following equation:

$$1/T_m - 1/T_m^{\infty} = 2RM_0/\Delta H_m M_n \tag{14}$$

where

$T_m^{\infty} = T_{melt}$ at infinite molecular weight
R = gas constant

Table XV. Primary Transition Temperatures of Selected PLA Copolymers [100]

Copolymer ratio	Glass transition temp. (°C)	Melting Temperature, (°C)
100/0 (L/D,L)-PLA	63	178
95/5 (L/D,L)-PLA	59	164
90/10 (L/D,L)-PLA	56	150
85/15 (L/D,L)-PLA	56	140
80/20 (L/D,L)-PLA	56	(125)[a]

[a]Melting point achieved by strain crystallization.

Table XVI. Effect of Temperature on the Molecular Weight of 90/10 PLA Copolymer [100]

Initial molecular weight	M_w after 30 min at 160°C	M_w after 30 min at 190°C
151,000 (M_n)	102,000	84,000
255,000 (M_w)	160,000	104,000
285,000 (M_z)	204,000	142,000
470,000 (M_n)	354,000	228,000
562,000 (M_w)	362,000	223,000
950,000 (M_z)	650,000	390,000

Table XVII. Effect of Processing Conditions on the Mechanical Properties of PLA Copolymers [100]

Copolymer Ratio, (L/D,L)-PLA	Process condition	Tensile strength, MPa	Young's modulus, GPa	Elongation (percent)	M_w
100/0	Injection molded, crystallized	64.8	4.00	—	800,000
90/10	Injection molded, amorphous	53.4	1.03	4.6	—
90/10	Injection molded, crystallized	58.6	1.29	5.1	—
90/10	Extruded, biaxially oriented, strain crystallized	80.9	3.41	41.2	145,000
90/10	Extruded, biaxially oriented, strain crystallized, heat set	70.1	2.76	20.7	145,000
95/5	Extruded, biaxially oriented, strain crystallized	68.6	1.88	56.7	120,000
95/5	Extruded, biaxially oriented, strain crystallized, heat set	60.7	1.63	63.8	120,000
80/20	Injection molded, amorphous	51.7	2.10	5.7	268,000
80/20	Extruded, biaxially oriented, strain crystallized	84.1	2.94	18.2	268,000
80/20	Extruded, biaxially oriented, strain crystallized, heat set	80.1	2.54	32.3	268,000

M_0 = molecular weight of the repeat unit
ΔH_m = heat of fusion per mole of the repeat unit

A plot of $1/T_m$ versus $1/M_n$ should give a straight line with a slope of $2RM_0/\Delta H_m$ and an intercept of $1/T_m^{\infty}$. This plot holds well for polymers of high molecular weight. The T_m and ΔH_m values obtained were 184°C and 3.5 kcal/mol, respectively, for PLLA [3].

Numerous dilute-solution viscosity experiments were performed on poly(lactic acid). Publications regarding poly(lactic acid) usually report a viscosity-average molecular weight. The literature reports numerous Mark–Houwink equations for poly(lactic acid). The Mark–Houwink constants are a function of the type of poly(lactic acid) used, the solvent used, and the temperature of the solution. Table XVIII presents dilute-solution viscosity data for various poly(lactic acid) polymers.

The rheological properties of PLA, especially the shear viscosity, have important effects on thermal processes, such as injection molding, extrusion, film blowing, sheet forming, fiber spinning, and thermoforming. Polylactide melts are shear thinning, similar to polystyrene. The melt viscosities of high-molecular-weight PLA are 5,000 to 10,000 poise (500–1000 Pa-s) at 10 to 50 reciprocal seconds. The weight-average molecular weights (M_w) of these PLA grades, determined by gel permeation chromatography (GPC), are about 100,000 for injection molding to about 300,000 for cast-extruded film grades. The molecular weights and the amounts of plasticizer govern the usable melt viscosities required for melt processing [5]. As previously mentioned, PLA undergoes thermal degradation at temperatures above 200°C (392°F). The working temperature is dependent on the melt viscosity, which is, in turn, dependent on the weight-average molecular weight of PLA, the amount of plasticizer, the shear rate, the type of melt processing, and the amount of work put into the polymer [5].

Table XVIII. Mark–Houwink Constants for Poly(Lactic Acid) in Selected Solvents (K = dl/g)

1. PLLA	$[\eta] = 5.45 \times 10^{-4} M_v^{0.73}$	25°C in chloroform [96, 110]
2. PDLLA	$[\eta] = 2.21 \times 10^{-4} M_v^{0.77}$	25° C in chloroform [96, 110]
3. PDLLA	$[\eta] = 1.29 \times 10^{-5} M_v^{0.82}$	25°C in chloroform [97]
4. Linear PLLA	$[\eta] = 4.41 \times 10^{-4} M_w^{0.72}$	25°C in chloroform [113]
5. "Star" PLLA (6 arms)	$[\eta] = 2.04 \times 10^{-4} M_w^{0.77}$	25°C in chloroform [113]
6. PDLLA	$[\eta] = 2.59 \times 10^{-4} M_v^{0.689}$	35°C in THF (iterative using GPC) [115]
7. PDLLA	$[\eta] = 5.50 \times 10^{-4} M_v^{0.639}$	31.15°C in THF (iterative using GPC) [115]
8. PLLA (amorphous)	$[\eta] = 6.40 \times 10^{-4} M_v^{0.68}$	30°C in THF [4]
9. PLLA (amor./semicryst.)	$[\eta] = 8.50 \times 10^{-4} M_v^{0.66}$	30°C in THF [4]
10. PLLA (semicryst.)	$[\eta] = 1.00 \times 10^{-3} M_v^{0.65}$	30°C in THF [4]
11. PDLLA	$[\eta] = 2.27 \times 10^{-4} M_v^{0.75}$	30°C in Benzene [116–118]
$[\eta] = \frac{2^{1/2}(\text{nsp} - \ln \eta\text{rel})^{1/2}}{C\ (\text{g/dl})}$	(one-point method)	Tuan–Fuoss viscometer
12. PDLLA	$[\eta] = 6.06 \times 10^{-4} M_v^{0.64}$	25°C in chloroform [118]
13. PLLA	$[\eta] = 5.72 \times 10^{-4} M_v^{0.72}$	30°C in Benzene [118]
14. PDLLA	$[\eta] = 1.58 \times 10^{-4} M_n^{0.78}$	25°C in ethyl acetate [119]
15. PDLLA	$[\eta] = 1.63 \times 10^{-4} M_w^{0.73}$	25°C in ethyl acetate [119]

Note: The PDLLA supplied by Cargill is insoluble in sequencer-grade ethyl acetate.

Table XIX. Power-Law Equations for Poly(D,L-Lactic Acid)

PLA	Temperature (°C)	Equation	r^2
Amorphous	150°C	$\eta = 649{,}386\gamma^{-0.8332}$	0.9984
Amorphous	170°C	$\eta = 242{,}038\gamma^{-0.7097}$	0.9980
Semicrystalline	150°C	$\eta = 609{,}159\gamma^{-0.8134}$	0.9992
Semicrystalline	170°C	$\eta = 241{,}721\gamma^{-0.7031}$	0.9982

Fang and Hanna [120] studied the rheological properties of amorphous and semicrystalline poly(lactic acid) using a tube rheometer on an extruder. Two types of PLA resins (amorphous and semicrystalline) at 150°C and 170°C, and at various shear rates (30, 50, 70, 90, 110, 130, and 150 rpm screw speed), were analyzed. The viscosity data was calculated from the pressure profiles and the volumetric flow rate. The melt viscosity was investigated as a function of resin type, temperature, and shear rate. Under the same processing conditions, semicrystalline PLA had a higher shear viscosity than amorphous PLA. As the temperature increased, the shear viscosity decreased for both types of PLA. The PLA melt was characterized as a pseudoplastic, non-Newtonian fluid. Power-law equations were used to describe the behavior of the PLA melts [120] (Table XIX).

A summary of the research is described as follows. The PLA was obtained from Cargill. Both samples had a number-average molecular weight of 88,000 g/mole. The amorphous PLA had a D- to L-lactide ratio of 18 to 82, and the semicrystalline PLA had a D- to L-lactide ratio of 5 to 95 [120]. A single-screw Brabender extruder with an L/D and compression ratio of 20/1 and 3:1, respectively, was used. Fang and Hanna [120] presented two equations that related density of the PLA melt to the volumetric flow rate and the PLA melt temperature, T_{melt}. These equations are as follows:

$$Q = m/\rho \tag{15}$$

where

Q = volumetric flow rate (m^3/sec)
m = mass flow rate (kg/sec)
ρ = density of the PLA melt (kg/m^3)

$$\rho = \frac{1.1452}{1 + 0.0074(T_{melt} - 150)} \tag{16}$$

After conducting their experiments, Fang and Hanna [120] had used the power-law equation to present their data. The power-law equation can be expressed as follows:

Table XX. Peak Band Assignments for PLA Infrared Spectra [109, 122, 123]

Assignment	Peak position, cm^{-1}
—OH stretch (free)	3571
—CH— stretch	2995 (asym.), 2944 (sym.)
—C=O carbonyl stretch	1759
—CH_3 bend	1453
—CH—deformation including sym. and asym. bend	1382, 1362
—C=O bend	1268
—C—O— stretch	1194, 1130, 1093
—OH bend	1047
—C—C— stretch	926, 868

$$\eta = m\gamma^{n-1} \tag{17}$$

where

η = melt viscosity (Pa-sec)
γ = shear rate (sec^{-1})
m = consistency factor
n = flow index ($n > 1$, dilatant; $n = 1$, Newtonian; $n < 1$, pseudoplastic)

Table XIX summarizes the power-law equations for PLA melt viscosity [120]. Melt flow index data of poly(lactic acid) can be found in the literature [31]. A plot of melt flow rate versus molecular weight is shown.

Nuclear magnetic resonance (NMR) data of PLA is presented in the literature [4, 31]. Of particular interest is the carbonyl region centered at 169 ppm. Poly(lactic acid) produced by condensation polymerization has five characteristic peaks at 169.27, 169.31, 169.42, 169.49, and 169.66. The signal at 169.66 ppm can be assigned to the carbonyl carbon atom of successive L-lactic acid units due to large intensities. The other four small signals—at 169.27, 169.31, 169.42, and 169.49 ppm—can be assigned to carbonyl carbons influenced by D-lactic acid units in the polymer sequence. The differences in the pattern of these signals are attributed to the differences in the polymer sequence [31]. In condensation polymerization, the L- and D-lactic acid are introduced at random, whereas in ring-opening polymerization, they are introduced in pairs. Spinu et al. [4] showed one peak at 173.75 ppm for an L/D-PLA "as polymerized" stereocomplex and an L,D-PLA random copolymer from racemic lactide having six peaks. These peaks are at 169.136, 169.301, 169.342, 169.400, 169.548, and 169.569 ppm.

Infrared spectroscopy data of poly(lactic acid) is presented in the literature, and the data is presented in Table XX [121, 122]. A more detailed table of IR and Raman spectroscopy frequencies can be found in the

literature for semicrystalline and amorphous PLLA [124, 125]. The reported frequencies, and their corresponding vibrational mode assignments, range from 60 to 2995 cm^{-1} for both infrared and Raman spectroscopy. Younes and Cohn [121] reported two bands that are related to the crystalline and the amorphous phase of PLA. They can be found at 755 cm^{-1} and 869 cm^{-1}. The peak at 755 cm^{-1} can be assigned to the crystalline phase, while the peak at 869 cm^{-1} can be assigned to the amorphous phase.

The ultraviolet spectrum of poly(lactic acid) is presented in the literature. Lalla and Chugh [109] dissolved PLA in choloroform and measured the wavelength at which the maximum absorbance occurred. They found this to be at 240 nm and attributed this to the ester group present in the polymer. Gupta and Deshmukh [117] dissolved PLA in benzene and investigated the degradation of PLA using UV spectroscopy. The $n \rightarrow \pi^*$ transition characteristic of undegraded PLA occurs at 287 nm, whereas on degradation there is a blue shift, and the absorption band occurs at 280 nm, suggesting that the carbonyl carbon-oxygen bond cleavage is more efficient than other cleavages, which would result in the formation of —COOH groups on the polymer chain ends. This cleavage will decrease the number of ester linkages and increase the number of carboxyl end-groups, resulting in an increase in the melting temperature of PLA on degradation [117].

Tsuji *et al.* [126] measured the optical rotation of poly(D-lactic acid) and poly(L-lactic acid). The specific optical rotation, $[\alpha]$, of the polymers was measured in chloroform at a concentration of 1 g/dl at 25°C, using a Perkin-Elmer polarimeter 241 at a wavelength of 589 nm. The values of 156° and −153° were in good agreement to the reported values of 150° and −150° for PDLA and PLLA, respectively [126]. Perego *et al.* reported specific optical rotation $[\alpha]$ values of −157 to −160° for PLLA [110].

The solubility parameter of PLA is reported in the literature [127, 128]. Table XXI is a table from the literature [128] for poly(D,L-lactic acid). Gross *et al.* had reported a value of 11.25 $cal^{0.5} \times cm^2$ [127]. The value of the solubility parameter is most likely closer to that reported in the aforementioned tables.

Kim *et al.* [133] reported the mechanical properties of poly(L-lactic acid)/starch composites. The number and weight-average molecular weights of the PLLA were 190,000 and 360,000 g/mole, respectively. The mechanical properties of these composites were in close agreement to similar composites compounded at USDA-ARS-NCAUR. Table XXII summarizes the mechanical properties research by Kim. The blends were melt blended in a Brabender twin-crew extruder and the dogbone tensile bars were compression molded. Kim [133] indicated that the starch granules were incompatible with the PLLA matrix, based on scanning electron microscopy (SEM) micrographs. This is what was observed at the USDA-ARS-NCAUR. Thermal properties of the PLLA/starch composites were also reported.

Table XXI. Solubility Parameters of Poly(Lactic Acid)

Determination method	Solubility parameter ($cal^{0.5} \times cm^{-1.5}$)
Density in solution [128, 129]	10.25 ± 0.16
Density in solution [128, 130]	10.29 ± 0.13
Limiting viscosity number, $[\eta]$ [128, 129]	10.00 ± 0.20
Limiting viscosity number, $[\eta]$ [128, 130]	10.05 ± 0.23
Increment Methods	
Small [127, 129]	9.7
Hoy [127, 129]	9.9
Van Krevelen [127, 131]	9.4
Fedors [127, 132]	11.1

Kim [133] reported the results of thermal degradation of PLLA and PLLA/starch composites, determined by thermogravimetric analysis (TGA). For PLLA, thermal decomposition began at 310°C and was completed by 400°C. For the PLLA/cornstarch composite, the onset of decomposition was at 220°C–230°C, with most of the decomposition occurring between 280°C and 340°C. The greater the cornstarch content in the composite, the lower the thermal degradation onset temperature [133].

Kim [133] reported water immersion data for PLLA and PLLA/cornstarch composites. After 50 days of immersion, PLLA picked up 1% moisture, whereas the PLLA/cornstarch composites picked up 6 to 8% moisture, by weight, depending on the composite. The moisture absorption was proportional to the starch content of the composite.

Finally, Kim [133] reported tensile and thermal properties of PLLA/starch/plasticizer composite films. Table XXIII shows what Kim reported [133].

Park *et al* [123] reported the thermal properties of poly(L-lactic acid)/cornstarch and six-armed star PLA/cornstarch composites. The molecular weights of the PLLA and the star-shaped PLA were 367,000 and 61,000 g/mole, respectively. Tables XXIV and XXV summarize the thermal analysis (differential scanning calorimetry) study by Park [123].

The maximum peak temperatures (onset for T_g) and the heats of fusion in the DSC thermograms for the PLA/cornstarch composites are denoted in Tables XXIV and XXV. When starch was added, the glass-transition temperatures of both L-PLA and star-PLA/cornstarch

Table XXII. Mechanical Properties of Composites Containing Cornstarch (CS) and High Amylose Cornstarch (HACS) [133]

Polymer	Tensile strength (MPa)	Elongation at break (%)	Modulus (GPa)	Toughness	Impact strength (kg-f/cm)
PLLA	60.00	3.1	2.5	0.93	125.6
PLLA/CS 93/7	48.5	3.1	2.5	0.75	130.8
PLLA/CS 84/16	48.7	2.6	2.8	0.63	131.8
PLLA/CS 79/21	49.5	2.5	2.8	0.62	120.7
PLLA/CS 70/30	46.5	2.4	3.2	0.56	110.0
PLLA/CS 60/40	38.5	2.0	3.0	0.39	98.0
PLLA/HACS 84/16	61.5	2.6	3.1	0.80	
PLLA/HACS 79/21	59.0	2.5	3.1	0.74	
PLLA/HACS 70/30	54.0	2.2	3.4	0.59	
PLLA/HACS 60/40	45.4	2.0	3.2	0.45	

Table XXIII. Mechanical Properties of Starch–PLA Composites Containing Selected Plasticizers

Blend	Tensile strength (MPa)	Elongation at break (%)	Modulus (GPa)	T_g (°C)	T_m (°C)	ΔH_f (J/g)
80:20 PLLA/starch	48.0	2.5	2.8	59.0	172.1	43.4
+5% PCL	40.0	3.1	2.0	55.7	171.1	31.6
+5% PEG400	30.8	3.0	1.1	49.4	169.2	39.3
+5% Glycerol	30.3	4.7	0.7	49.9	168.8	44.7
+5% Lauryl Alcohol	20.5	1.5	1.3	47.0	169.0	45.1

Note: PCL: polycaprolactone; PEG400: poly(ethylene glycol).

composites remained almost unchanged, but the crystallization characteristics were influenced. In the case of the PLLA/cornstarch composite, the width of the crystallization peaks became narrower, and the maximum crystallization temperatures shifted to lower temperatures. These results were indicative of an increase in crystallization rate. The enthalpies of crystallization and melting became larger as the starch content increased. This suggested that starch played a role as a nucleating agent. In the case of the star-PLA/cornstarch composite, both the crystallization and the melting temperatures were the lowest at a starch content of 5 wt% and shifted to higher temperatures as the starch content exceeded 5%. The enthalpies of crystallization and melting were a maximum at a 5% starch content, and they decreased as the starch content increased above 5%. This indicated that starch acted as a nucleating agent for the star-PLA, enhancing its crystallinity. This effect diminished when the starch content exceeded 5%. It was suggested that at a high starch level, the starch aggregated, the particle sizes of starch aggrega-

Table XXIV. Thermal Properties of Poly(L-Lactic Acid)/Cornstarch Composites, Determined by Differential Scanning Calorimetry

Starch content (wt%)	T_g (°C)	$T_{crystal}$ Temperature (°C)	$T_{crystal}$ $\Delta H_{crystal}$ (J/g)	T_{melt} Temperature (°C)	T_{melt} ΔH_{melt} (J/g)
0	56.8	121.8	41.0	168.7	42.4
5	56.5	105.0	41.1	167.8	44.8
10	57.0	104.2	42.4	169.0	48.0
15	57.0	104.4	45.4	167.8	50.6
20	56.8	105.2	48.7	170.0	54.5
30	56.8	105.0	54.9	170.0	62.0

Table XXV. Thermal Properties of Poly(Star-Lactic Acid)/Cornstarch Composites, Determined by Differential Scanning Calorimetry

Starch content (wt%)	T_g (°C)	$T_{crystal}$ Temperature (°C)	$T_{crystal}$ $\Delta H_{crystal}$ (J/g)	T_{melt} Temperature (°C)	T_{melt} ΔH_{melt} (J/g)
0	52.8	128.4	—	149.9	—
5	52.0	114.6	8.2	143.8	8.6
10	52.5	116.0	7.8	144.0	8.2
15	52.3	116.7	8.0	143.7	8.2
20	52.2	124.3	6.6	145.8	7.0
30	53.1	125.4	3.7	147.3	4.7

tion became larger, and consequently, the large starch particles prevented crystal growth. The overall influence of the starch addition on star-PLA was larger than that of L-PLA/starch composites [123].

Park *et al.* [123] had investigated the morphology of the PLLA- and the star-PLA/cornstarch composites using microscopy. Spherulites of PLLA and star-PLA were grown radially at 110°C and analyzed by optical microscopy. The average spherulite radius was 120 μm and 140 μm for pure star-PLA and PLLA, respectively [123]. The size and shape of the spherulite was dependent on starch content in the composite. As the starch content increased, the spherulite size decreased and became more irregular in shape. This suggested that starch may play a role as a nucleating agent for PLA. Scanning electron microscopy revealed good adhesion of the starch granules to the PLA matrix up to 5% starch content. As the starch content increased, voids appeared, which were formed as the separation of the starch and the matrix proceeded. In the case of the star-PLA/cornstarch composites, the voids were more easily observed and were larger than in the case of the PLLA/cornstarch composites [123].

The relative mechanical properties of the PLA/cornstarch composites were studied using the Nielsen and Nicolais–Narkis equations. These equations relate filler content in the composite to the elongation and tensile strength of the composite, respectively. The Nielsen equation is as follows:

$$\epsilon_{comp} = \epsilon_0[1 - (\phi_f)^{1/3}] \quad (18)$$

In this equation ϵ_{comp} and ϵ_0 are the elongation to break of the composite and the matrix, respectively. The volume fraction of the filler (starch) is ϕ_f. The Nielsen equation assumes that the filler particles are spherical, the matrix is homogeneous, and there is perfect adhesion between the matrix and the filler. The Nicolais–Narkis equation is as follows:

$$\sigma_{comp} = \sigma_0[1 - 1.21(\phi_f)^{1/3}] \quad (19)$$

In this equation, σ_{comp} and σ_0 are the ultimate tensile strengths of the composite and the matrix, respectively. The volume fraction of the filler (starch) is ϕ_f. The Nicolais–Narkis equation assumes that the filler particles are spherical, the matrix is homogeneous, and there is no adhesion between the matrix and the filler. The relative mechanical properties showed that some adhesion existed between PLA and the starch granules, but the adhesion was poor. An increase in the starch content resulted in a reduction of tensile strength and elongation of the composites. The star-PLA had shown a slightly better adhesion to the starch granules than the PLLA, but the adhesion was still poor.

Table XXVI. Mechanical Properties of Composites Containing Cornstarch and Wheat Starch with Various Blending Ratios

Composite	Tensile strength (MPa)	Elongation at break (%)	Modulus (GPa)
PLLA	61 ± 1.07	6.33 ± 0.33	1.204 ± 0.132
Cornstarch and PLLA			
20:80	42.4 ± 2.7	2.9 ± 0.24	1.613 ± 0.054
40:60	33 ± 1.04	2.44 ± 0.18	1.496 ± 0.153
50:50	32.4 ± 3.4	2.15 ± 0.21	1.633 ± 0.088
60:40	23.9 ± 1.5	1.52 ± 0.10	1.734 ± 0.142
70:30	18.9 ± 0.43	1.10 ± 0.09	1.832 ± 0.110
80:20	13.2 ± 2.4	0.84 ± 0.16	1.739 ± 0.059
Wheat starch and PLLA			
20:80	44.7 ± 3.8	3.96 ± 0.2	1.327 ± 0.152
40:60	41.2 ± 3.8	2.96 ± 0.17	1.551 ± 0.158
50:50	35.9 ± 1.8	2.39 ± 0.11	1.669 ± 0.092
60:40	29.7 ± 1.2	1.94 ± 0.08	1.661 ± 0.105
70:30	22.3 ± 1.5	1.19 ± 0.13	1.954 ± 0.192
80:20	16.4 ± 1.3	1.12 ± 0.15	1.594 ± 0.140

Sun *et al.* [134] reported the mechanical properties of poly(L-lactic acid)/starch composites. The reported molecular weight of the PLLA was 120,000 g/mole. A comparison was made between corn and wheat starches. The mechanical properties of these composites were in close agreement to similar composites compounded at USDA-ARS-NCAUR. Table XXVI is a summary of the mechanical properties of the composites [134].

The composites were melt blended in a Haake twin-screw extruder, and dogbone tensile bars were compression molded. The relative mechanical properties of the PLLA/starch composites were studied using the Nielsen and Nicolais–Narkis equations. The relative mechanical properties showed that some adhesion existed between PLA and the starch granules, but the adhesion was poor. An increase in the starch content resulted in a reduction of tensile strength and elongation of the composites. The wheat starch had shown a slightly better adhesion to the PLLA than did the cornstarch, but the adhesion was still poor. This was evident in the fact that the wheat starch had shown a slightly greater slope than that of the cornstarch for both the Nielsen and Nicolais–Narkis plots. This might have been caused by the variations in starch granular size and shape. The average granular size of wheat starch was greater than that of cornstarch, so the contact surface area at the interface between PLA and wheat starch would be larger than that between PLA and cornstarch. The adhesion forces between PLA and starch may be due to polar interactions between the two phases

and hydrogen bonding between the carbonyl group of PLA and the hydroxyl group of starch.

Sun [134] indicated that the starch granules were incompatible with the PLLA matrix, based on SEM micrographs. Some gaps existed between the starch granules and PLLA at all weight ratios. The PLA phase became discontinuous when the starch content increased to ≥60%, and at 80% starch, the starch granules were not covered by the PLA phase. This is what was observed at the USDA-ARS-NCAUR, but starch contents greater than 70% weren't investigated. The cornstarch granules were on the order of 10 μm. They were round and angular in shape. The wheat starch granules were about 10–20 μm in size. The granules were oval shaped. The starch granules maintained their shape despite being subjected to heat and mechanical shear in the extruder.

Thermal properties of the PLLA/starch composites were also reported. The glass-transition, crystallization, and melt temperatures of the PLLA were 60°C, 125.2°C, and 172°C, respectively [134]. The crystallinity was reported to be 3.9%. The following equation was used to calculate the percentage crystallinity of PLLA in the blends [134]:

$$X_c(\%) = (\Delta H_m + \Delta H_{ci}) \times 100/(93 \times X_{\mathrm{PLA}}) \qquad (20)$$

where ΔH_m and ΔH_{ci} are the enthalpies (J/g) of fusion and crystallization of the composite, respectively; 93 J/g is the enthalpy of fusion of a PLA crystal of infinite size; and X_{PLA} is the weight fraction of PLA. In a comparison between corn and wheat starch at a particular weight ratio, there were no significant differences in the glass-transition, crystallization, and melt temperatures, respectively. In contrast to Park *et al.* [123], the crystallization temperatures of the composites were not affected by the starch contents. Park [123] reported a decrease in the crystallization temperature with an increase in the starch content. The lowest PLLA crystallinities occurred at 60% cornstarch and 50% wheat starch [134]. The difference between corn and wheat starch might be caused by the difference in starch granule shape and size as well as size distribution.

REFERENCES

1. M. H. Hartmann (1998) in D. L. Kaplan (Ed.), *Biopolymers from Renewable Resources*, Springer-Verlag, Berlin, pp. 367–411.
2. R. E. Conn, J. J. Kolstad, J. F. Borzelleca, D. S. Dixler, L. J. Filer, B. N. LaDu, and M. W. Pariza (1995) *Food Chemistry and Toxicology* **33**(4), 273–283.
3. K. Jamshidi, S. H. Hyon, and Y. Ikada, (1988) *Polymer* **29,** 2229–2234.
4. M. Spinu, C. Jackson, M. Y. Keating, and K. H. Gardner (1996) *Journal of Macromolecular Science—Pure and Applied Chemistry* **A33**(10), 1497–1530.
5. R. G. Sinclair (1996) *Journal of Macromolecular Science—Pure and Applied Chemistry* **A33**(5), 585–597.
6. H. Benninga (Ed.) (1990) *A History of Lactic Acid Making*, Kluwer Academic Publishing, Boston, London, Dordrecht.
7. J. H. Van Ness (1981) in *Kirk-Othmer Encyclopedia of Chemical Technology*, 3rd ed., Vol. 13, John Wiley and Sons, New York, pp. 80–103.
8. R. Datta, S. Tsai, P. Bonsignore, S. Moon, and J. Frank (1995) *FEMS Microbiology Reviews* **16,** 221–231.
9. G. B. Kharas, F. Sanchez-Riera, and D. K. Severson (1994) in D. P. Mobley (Ed.), *Plastics From Microbes*, Hanser-Gardner, Munich, pp. 93–137.
10. K. Enomoto, M. Ajioka, and A. Yamaguchi (1994) U.S. Patent 5,310,865.
11. T. Kashima, T. Kameoka, C. Higuchi, M. Ajioka, and A. Yamaguchi (1995) U.S. Patent 5,428,126.
12. F. Ichikawa, M. Kobayashi, M. Ohta, Y. Yoshida, S. Obuchi, and H. Itoh (1995) U.S. Patent 5,440,008.
13. M. Ohta, Y. Yoshida, S. Obuchi (1995) U.S. Patent 5,444,143.
14. B. Buchholz (1994) U.S. Patent 5,302,694.
15. L. Cotarca, P. Delogu, A. Nardelli, and V. Sunjic (1996) *Synthesis* **5,** 553–576.
16. J. Seppala, J. F. Selin and T. Su (1993) European Patent 593,271.
17. J. Seppala, J. F. Selin, T. Su (1995) U.S. Patent 5,380,813.
18. M. Harkonen, K. Hiltunen, M. Malin, and J. V. Seppala (1995) *Journal of Macromolecular Science—Pure and Applied Chemistry* **A32**(4), 857–862.
19. P. V. Bonsignore (1995) U.S. Patent 5,470,944.
20. M. Spinu (1993) U.S. Patent 5,270,400.
21. A. C. Ibay and L. P. Tenney (1993) U.S. Patent 5,206,341.
22. J. Kylma, M. Harkonen, and J. V. Seppala (1995) *Abstracts of the Fourth International Workshop on Biodegradable Polymers*, Poster 38.
23. H. Inata and S. Matsumura (1985) *Journal of Applied Polymer Science* **30**(8), 3325–3337.
24. S. M. Aharoni and T. Largman (1983) U.S. Patent 4,417,031.
25. C. D. Dudgeon (1976) *Bis-Orthoesters as Polymer Intermediates*, Thesis, University of Massachusetts.
26. S. M. Aharoni and D. Masilamani (1986) U.S. Patent 4,568,720.
27. S. M. Aharoni, C. E. Forbes, W. B. Hammond, D. M. Hindenlang, F. Mares, K. O'Brien, and R. D. Sedgwick (1986) *Journal of Polymer Science, Part A: Polymer Chemistry Edition* **24**(6), 1281–1296.
28. A. J. Pennings and S. Gogolewski (1982) *Die Makromolekulare Chemie, Rapid Communications* **3**(12), 839–845.
29. J. Lunt (1998) *Polymer Degradation and Stability* **59,** 145–152.
30. M. Ajioka, K. Enomoto, K. Suzuki, and A. Yamaguchi (1995) *Journal of Environmental Polymer Degradation* **3**(4), 225–234.
31. M. Ajioka, K. Enomoto, K. Suzuki, and A. Yamaguchi (1995) *Bulletin of the Chemical Society of Japan* **68**(8), 2125–2131.
32. H. Suizu, M. A. Takagi, A. Yamaguchi, and M. Ajioka (1996) U.S. Patent 5,496,923.
33. W. H. Carothers, G. L. Dorough, and F. J. Van Natta (1932) *Journal of the American Chemical Society* **54,** 761–772.
34. C. E. Lowe (1954) U.S. Patent 2,668,162.
35. H. R. Kricheldorf and I. Kreiser (1987) *Die Makromolekulare Chemie* **188,** 1861–1873.
36. H. R. Kricheldorf and M. Sumbel (1989) *European Polymer Journal* **25**(6), 585–591.
37. V. W. Dittrich and R. C. Schulz (1971) *Die Angewandte Makromolekulare Chemie* **15,** 109–126.
38. H. R. Kricheldorf and R. Dunsing (1986) *Die Makromolekulare Chemie* **187**(7), 1611–1625.
39. Z. Jedlinski, W. Walach, P. Kurcok, and G. Adamus (1991) *Die Makromolekulare Chemie* **192**(9), 2051–2057.

40. P. Kurcok, A. Matuszowicz, Z. Jedlinski, H. R. Kricheldorf, Ph. Dubois, and R. Jerome (1995) *Macromolecular Rapid Communications* **16,** 513–519.
41. H. R. Kricheldorf and I. Kreiser-Saunders (1990) *Die Makromolekulare Chemie* **191**(5), 1057–1066.
42. H. R. Kricheldorf and C. Boettcher (1993) *Journal of Macromolecular Science—Pure and Applied Chemistry* **A30,** 441–448.
43. H. R. Kricheldorf and A. Serra (1985) *Polymer Bulletin* **14,** 497–502.
44. J. Kleine and H. Kleine (1959) *Die Makromolekulare Chemie* **30,** 23–38.
45. H. R. Kricheldorf and C. Boettcher (1993) *Die Makromolekulare Chemie, Macromolecular Symposia* **73,** 47–64.
46. R. Dunsing and H. R. Kricheldorf (1985) *Polymer Bulletin* **14,** 491–495.
47. H. R. Kricheldorf, I. Kreiser-Saunders, and N. Scharnagl (1990) *Die Makromolekulare Chemie, Macromolecular Symposia* **32,** 285–298.
48. L. Sipos, M. Zsuga, and T. Kelen (1992) *Polymer Bulletin* **27**(5), 495–502.
49. J. Dahlman, G. Rafler, K. Fechner, and B. Mehlis (1990) *British Polymer Journal* **23**(3), 235–240.
50. F. E. Kohn, J. W. A. Van Den Berg, G. Van De Ridder, and J. Feijen (1984) *Journal of Applied Polymer Science* **29**(12), 4265–4277.
51. E. Lillie and R. C. Schulz (1975) *Die Makromolekulare Chemie* **176(6),** 1901–1906.
52. G. Schwach, J. Coudane, R. Engel, and M. Vert (1994) *Polymer Bulletin* **32,** 617–623.
53. X. Zhang, U. P. Wyss, D. Pichora, and M. F. A. Goosen (1992) *Polymer Bulletin* **27**(6), 623–629.
54. A. Schindler, Y. M. Hibionada, and C. G. Pitt (1982) *Journal of Polymer Science, Polymer Chemistry Edition* **20**(2), 319–326.
55. J. Dahlmann and G. Rafler (1993) *Acta Polymerica* **44**(2), 103–107.
56. D. K. Gilding and A. M. Reed (1979) *Polymer* **20,** 1459–1464.
57. H. R. Kricheldorf, I. Kreiser-Saunders, and C. Boettcher (1995) *Polymer* **36**(6), 1253–1259.
58. X. Zhang, D. A. MacDonald, M. F. A. Goosen, and K. B. McAuley (1994) *Journal of Polymer Science, Part A: Polymer Chemistry Edition* **32**(15), 2965–2970.
59. A. J. Nijenhuis, D. W. Grijpma, and A. J. Pennings (1991) *Polymer Bulletin* **26**(1), 71–77.
60. A. J. Nijenhuis, D. W. Grijpma, and A. J. Pennings (1992) *Macromolecules* **25,** 6419–6424.
61. Y. J. Du, P. J. Lemstra, A. J. Nijenhuis, H. A. M. Van Aert, and C. Bastiaansen (1995) *Macromolecules* **28**(7), 2124–2132.
62. D. R. Witzke (1996) *Properties and Engineering of Polylactide Polymers*, Thesis, Michigan State University.
63. I. C. McNeill and H. A. Leiper (1985) *Polymer Degradation and Stability* **11**(4), 309–326.
64. T. G. Kulagina, B. V. Lebedev, Y. G. Kiparisova, Y. B. Lyudvig, and I. G. Barskaya (1982) *Polymer Science USSR* **24**(7), 1702–1708.
65. F. W. Van Der Weij (1980) *Die Makromolekulare Chemie* **181**(12), 2541–2548.
66. T. G. Kulagina, B. V. Lebedev, Y. G. Kiparisova, Y. B. Lyudvig, and I. G. Barskaya (1982) *Vysokomolekulyarnye Soedineniya Seriya* **A24,** 1496–1501.
67. H. R. Kricheldorf, S. R. Lee, and S. Bush (1996) *Macromolecules* **29**(5), 1375–1381.
68. Y. Hori, Y. Takahashi, A. Yamaguchi, and T. Nishishita (1993) *Macromolecules* **26**(16), 4388–4390.
69. T. M. Abdel-Fattah and T. J. Pinnavaia (1996) *Chemical Communications* **5,** 665–666.
70. L. Trofimoff, T. Aida, and S. Inoue (1987) *Chemistry Letters* **5,** 991–994.
71. C. X. Song and X. D. Feng (1984) *Macromolecules* **17**(12), 2764–2767.
72. M. Bero, J. Kasperczyk, and Z. J. Jedlinski (1990) *Die Makromolekulare Chemie* **191**(10), 2287–2296.
73. H. R. Kricheldorf, M. Berl, and N. Scharnagl (1988) *Macromolecules* **21**(2), 286–293.
74. Ph. Dubois, C. Jacobs, R. Jerome, and Ph. Teyssie (1991) *Macromolecules* **24**(9), 2266–2270.
75. C. Jacobs, Ph. Dubois, R. Jerome, and Ph. Teyssie (1991) *Macromolecules* **24**(11), 3027–3034.
76. Ph. Dubois, R. Jerome, and Ph. Teyssie (1991) *Die Makromolekulare Chemie, Macromolecular Symposia* **42/43,** 103–116.
77. S. J. McLain, T. M. Ford, and N. E. Drysdale (1992) *Polymer Preprints* **33**(2), 463–464.
78. S. J. McLain and N. E. Drysdale (1991) U.S. Patent 5,028,667.
79. S. J. McLain and N. E. Drysdale (1992) U.S. Patent 5,095,098.
80. T. M. Ford and S. J. McLain (1993) U.S. Patent 5,208,297.
81. N. E. Drysdale, T. M. Ford, and S. J. McLain (1993) U.S. Patent 5,235,031.
82. T. M. Ford, and S. J. McLain (1994) U.S. Patent 5,292,859.
83. H. R. Kricheldorf, I. Kreiser-Saunders, C. Jurgens, and D. Wolter (1996) *Die Makromolekulare Chemie, Macromolecular Symposia* **103,** 85–102.
84. R. Vasanthakumari and A. J. Pennings (1983) *Polymer* **24**(2), 175–178.
85. B. Kalb and A. J. Pennings (1980) *Polymer* **21**(6), 607–612.
86. G. L. Loomis and J. R. Murdoch (1990) U.S. Patent 4,902,515.
87. G. L. Loomis and J. R. Murdoch (1988) U.S. Patent 4,719,246.
88. M. Spinu (1994) U.S. Patent 5,317,064.
89. Y. Ikada, H. Jamshidi, H. Tsuji, and S. H. Hyon (1987) *Macromolecules* **20**(4), 904–906.
90. N. Yui, P. J. Dijkstra, and J. Feijen (1990) *Die Makromolekulare Chemie* **191**(3), 481–488.
91. H. Tsuji, F. Horii, S. H. Hyon, and Y. Ikada (1991) *Macromolecules* **24**(10), 2719–2724.
92. H. Tsuji and Y. Ikada (1993) *Macromolecules* **26**(25), 6918–6926.
93. W. M. Stevels, M. J. K. Ankone, P. J. Dijkstra, and J. Feijen (1995) *Macromolecular Chemistry and Physics* **196,** 3687–3694.
94. E. W. Fischer, H. J. Sterzel, and G. Wegner (1973) *Kolloid-Z, u. Z. Polymere* **251,** 980–990.
95. H. Tsuji and Y. Ikada (1995) *Polymer* **36**(14), 2709–2716.
96. H. Tsuji and Y. Ikada (1996) *Polymer* **37**(4), 595–601.
97. J. Huang, M. S. Lisowski, J. P. Runt, E. S. Hall, R. T. Kean, N. Buehler, and J. S. Lin (1998) *Macromolecules* **31,** 2593–2599.
98. C. Marega, A. Marigo, V. DiNoto, and R. Zannetti (1992) *Die Makromolekulare Chemie* **193,** 1599–1606.
99. W. Hoogsteen, A. R. Postema, A. J. Pennings, and G. ten Brinke (1990) *Macromolecules* **23,** 634–642.
100. D. M. Bigg (1996) in *Society of Plastics Engineers—Annual Technical Conference* **54**(2), 2028–2039.
101. S. Mazzullo, G. Paganetto, and A. Celli (1992) *Progress in Colloid and Polymer Science* **87,** 32–34.
102. C. Migliaresi, A. De Lollis, L. Fambri, and D. Cohn (1991) *Clinical Materials* **8,** 111–118
103. Jeffrey J. Kolstad (1996) *Journal of Applied Polymer Science* **62,** 1079–1091.
104. R. Von Oepen and W. Michaeli (1992) *Clinical Materials* **10,** 21–28
105. J. Huang, N. Buehler, E. Hall, R. Kean, J. Kolstad, L. Wu, and J. Runt (1996) *Polymer Preprints* **37**(2), 370–371.
106. K. Kishore, R. Vasanthakumari, and A. J. Pennings (1984) *Journal of Polymer Science: Polymer Physics Edition* **22**(4), 537–542.
107. K. Kishore and R. Vasanthakumari (1988) *Colloid and Polymer Science* **266,** 999–1002.
108. E. Urbanovici, H. A. Schneider, and H. J. Cantow (1997) *Journal of Polymer Science: Part B: Polymer Physics* **35**(2), 359–369.
109. J. K. Lalla and N. N. Chugh (1990) *Indian Drugs* **27**(10), 516–522.
110. G. Perego, G. D. Cella, and C. Bastioli (1996) *Journal of Applied Polymer Science* **59,** 37–43.
111. M. H. Naitove (1995) *Plastics Technology* **41**(3), 15–17.

112. A. G. Mikos, A. J. Thorsen, L. A. Czerwonka, Y. Bao, R. Langer, D. N. Winslow, and J. P. Vacanti (1994) *Polymer* **35**(5), 1068–1077.
113. Y. Doi and K. Fukuda (Eds.) (1994) in *Biodegradable Plastics and Polymers*, Elsevier Science, New York, pp. 464–469.
114. C. Migliaresi, D. Cohn, A. DeLollis, and L. Fambri (1991) *Journal of Applied Polymer Science* **43**(1), 83–95.
115. J. A. P. P. Van Dijk, J. A. Smit, F. E. Kohn, and J. Feijen (1983) *Journal of Polymer Science: Polymer Chemistry Edition* **21**(1), 197–208.
116. M. C. Gupta and V. G. Deshmukh (1982) *Colloid and Polymer Science* **260**(3), 308–311.
117. M. C. Gupta and V. G. Deshmukh (1982) *Colloid and Polymer Science* **260**(5), 514–517.
118. A. Schindler and D. Harper (1979) *Journal of Polymer Science: Polymer Chemistry Edition* **17,** 2593–2599.
119. K. Xu, A. Kozluca, E. B. Denkbas, and E. Piskin (1996) *Journal of Applied Polymer Science* **59**(3), 561–563.
120. Q. Fang and M. A. Hanna (1999) *Industrial Crops and Products* **10**(1), 47–53.
121. H. Younes and D. Cohn (1988) *European Polymer Journal* **24**(8), 765–773.
122. M. Agarwal, K. W. Koelling, and J. J. Chalmers (1998) *Biotechnology Progress* **14**(3), 517–526.
123. J. W. Park, D. J. Lee, E. S. Yoo, S. S. Im, S. H. Kim, and Y. H. Kim (1999) *Korea Polymer Journal* **7**(2), 93–101.
124. G. Kister, G. Cassanas, M. Vert, B. Pauvert, and A. Terol (1995) *Journal of Raman Spectroscopy* **26**(4), 307–311.
125. G. Kister, G. Cassanas, and M. Vert (1998) *Polymer* **39**(2), 267–273.
126. H. Tsuji, Y. Ikada, S-H. Hyon, Y. Kimura, and T. Kitao (1994) *Journal of Applied Polymer Science* **51**(2), 337–344.
127. G. Rocha, R. A. Gross, and S. P. McCarthy (1992) *Polymer Preprints* **33**(2), 454–456.
128. U. Siemann (1992) *European Polymer Journal* **28**(3), 293–297.
129. J. Brandrup and E. H. Immergut (1975) *Polymer Handbook*, 2nd edn., Wiley Intersciences, New York.
130. C. M. Hansen (1967) *Journal of Paint Technology* **39,** 104–117.
131. A. F. M. Barton (1983) *Handbook of Solubility Parameters*, CRC Press, Boca Raton, FL.
132. R. F. Fedors (1974) *Polymer Engineering and Science* **14**(2), 147–154.
133. S. H. Kim, I-J. Chin, J-S. Yoon, S. H. Kim, and J-S. Jung (1998) *Korea Polymer Journal* **6**(5), 422–427.
134. X. Sun and T. Ke (2000) *Cereal Chemistry* **77**(6), 761–768.